

## Chapter 2 Reduced Reactivity of Aged Gold Nanoparticles

### 2.1. Introduction

#### 2.1.1. Gold nanoparticles

Gold is one of the most ancient subjects of research in science history. Alchemists were probably the earliest chemists in the planet, whose early practice generated many of the fundamentals of modern inorganic chemistry. In the past three decades, the research of gold experienced renaissance within the developing context of ‘nanotechnology’. Nano materials have the size on the nanometre scale in at least one dimension. The term ‘nanotechnology’ is somewhat misleading since nano is not an independent technology. It reflects a group of new physical, chemical, biological, electronic, engineering and many other properties shown in materials on the nanometre-size<sup>1-3</sup>. These new properties are size and sometimes shape dependent<sup>4</sup>. Nobel Laureate Richard Feynman inspired the research in this field using his visionary lecture ‘There is plenty of room at the bottom<sup>5</sup>, in 1959. The research topic experienced rapid exploding after 1990s.

Nanoparticles are an assembly of atoms forming a particle shape which normally have the size ranging from 1 to 100 nm<sup>6</sup>. As most metal atoms have the size of 0.1 to 0.2 nm<sup>7</sup>, a nanoparticle typically contains several tens to several thousand metal atoms. Gold nanoparticles (AuNPs) are among the most important metal nanoparticles. Naked (*e.g.* uncoated) particles are not stable, therefore AuNPs are commonly protected by stabilizing ligands. Solubility of AuNPs largely depends on the polarity and hydrophilicity of the protecting ligand. Soluble AuNPs are also known as colloidal gold. The historical applications<sup>8</sup> of colloidal gold can be traced back to 5<sup>th</sup> century B.C. when it was used to colour ceramics and make ruby glass. After middle ages, the colloidal gold was used as a precious medicine to cure many diseases. Michael Faraday’s attempt in 1857 to make colloidal gold by reducing chloroaurate by phosphorus in a two-phase system<sup>9</sup> is a milestone in the history of

AuNPs. It is the first well-documented example of the synthesis protocol of AuNPs. In the 20<sup>th</sup> century, various synthetic methods of AuNPs were reported.<sup>10-13</sup>

### **2.1.2. Applications of AuNPs**

AuNPs are among the most popular metal nanoparticles due to their stability and fascinating properties. They have applications in very important fields such as catalysis and medicine.

#### **2.1.2.1. Catalysis**

The electron-rich core and high surface-area-to-volume ratio make AuNPs very effective in catalysis. However, for a long time, gold was considered to be inert and stable. Therefore gold was and still is used to make coins and jewellery as it is resistant to corrosion and oxidation. Bulk gold showed no catalytical effect.<sup>14</sup> The report<sup>15-19</sup> of supported AuNPs as highly effective catalysts by Haruta *et al.* in 1989 was thus surprising and is considered a breakthrough in this field. Since then, gold catalysts have been explored extensively in a number of homogenous and heterogeneous systems.<sup>20-24</sup>

#### **2.1.2.2. Bio-medical applications**

Owing to the good biocompatibility and non-toxic nature of AuNPs, they are widely used in biology and medicine. Nanotoxicology<sup>25-26</sup> has been studied increasingly due to the increasing importance of nanomaterials in medicine and biology. Under general consideration, the gold core is often regarded as non-toxic<sup>27</sup>, the toxicity of AuNPs often depends on the stabilizing ligand<sup>28</sup> and the size of AuNPs<sup>29</sup>. Low toxicity of AuNPs gives them much potential in different applications. For instance, the unusual optical properties of AuNPs (caused by excitation of the conduction electrons, known as the surface plasmon effect<sup>30</sup>), depend on the size, shape and dielectric properties of the particle, and thus can be utilized for bio-imaging<sup>31</sup> with optical microscopy. The size and shape dependent light absorption makes AuNPs of different colours, which can be used for labelling purposes<sup>32</sup>. The strong absorption

of light by AuNPs leads to heating of the particles. This effect was exploited in the plasmonic photothermal therapy (PPTT)<sup>33</sup> in cancer treatment. Apart from optical imaging, functionalized AuNPs were also explored as contrast agents in other imaging techniques including X-ray<sup>34-35</sup>, Magnetic Resonance Imaging (MRI)<sup>34, 36</sup> and fluorescence imaging<sup>37</sup>. AuNPs can be conjugated with drug or biomolecules and used as a delivery vehicle in various *in vivo* and *in vitro* systems<sup>38-40</sup>. The photothermal property of AuNPs can be used here to control drug release. A number of bioconjugates<sup>8</sup> of AuNPs with DNA, sugar, peptides *etc.* have also exhibited unique properties in molecular recognition and sensing<sup>41-46</sup>.

Such important applications of AuNPs in different fields originate from their size, versatility and usability. AuNPs can be made with the size of several nanometres, they are therefore among the smallest metal nanoparticles. The fascinating properties of AuNPs make them extremely versatile and thus generate many unique applications across disciplines. With the advantages AuNPs bring, they are also convenient to make and functionalize. Next sections consider the preparation and reactions of AuNPs.

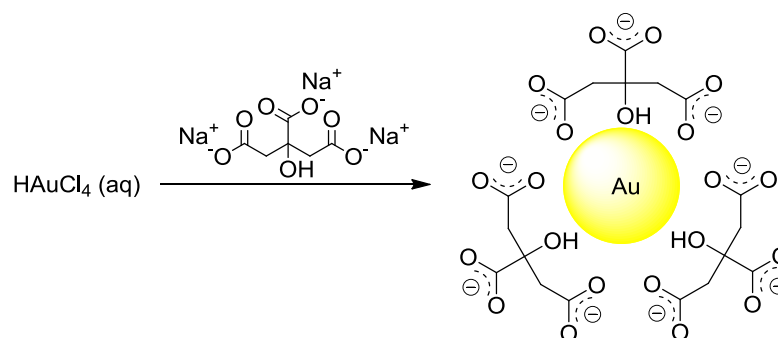
### 2.1.3. Synthesis of AuNPs

The synthesis of AuNPs is well-established in both aqueous solutions and organic solvents. Typically, gold salt (*e.g.* AuCl<sub>4</sub><sup>-</sup>) is reduced to Au(0) upon the introduction of a reducing agent, and nucleation of gold atoms leads to formation of a nanoparticle suspension. Without outer shell protection, naked AuNPs aggregate and coagulate to bulk gold. Hence, a stabilizing ligand is required to protect the nanoparticles by either absorption or covalent bonding to the gold surface.

#### 2.1.3.1. Citrate reduction method

Conventionally, citrate reduction is one of the most popular methods to synthesize AuNPs. The method was introduced by Turkevich in 1951<sup>13</sup> and typically used for synthesis of modestly polydisperse AuNPs in aqueous phase. In this method, trisodium citrate reduces Au(III) to Au(0). In the nucleation process, the citrate ions

and the oxidation products (*e.g.* acetone dicarboxylate) can also act as a surfactant to bind to the nanoparticles and therefore the AuNPs are stabilized by electrostatic repulsion (Scheme 2.1). As the protecting ligand, citrate ion is adsorbed on the gold surface, thus this method is typically used to synthesize AuNPs with a loose shell of ligand.



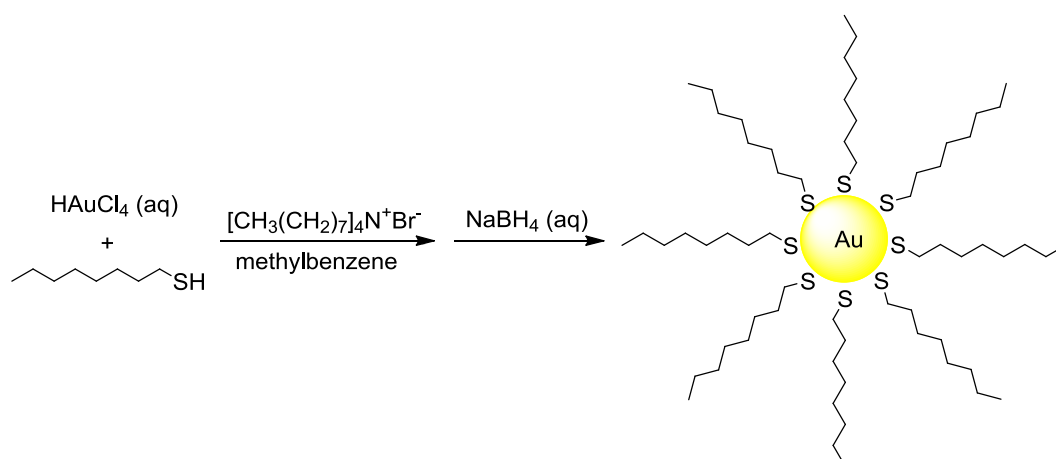
**Scheme 2. 1. Synthesis of AuNPs in aqueous solution by reducing hydrogen tetrachloroaurate (HAuCl<sub>4</sub>) with trisodium citrate.**

The mechanism of AuNP formation in this method was studied by many researchers and different reaction pathways were identified<sup>47-49</sup>. The original Turkevich's method resulted in AuNPs *ca.* 20 nm in diameter. Frens<sup>11</sup> reviewed this method in 1973 and reported that the particle size could be tuned by changing citrate/gold ratio. A recent report by Ji *et al.*<sup>47</sup> suggested that pH of the solution played an important role in the formation of AuNPs and in controlling the particle size. In the citrate reduction method, the AuNPs formed are protected by solvent molecules and electric charges which are provided by the citrate ions adsorbed on the surface of the gold core. Hence, the particles are only stable in solution.

### 2.1.3.2. Brust-Schiffrin method

The AuNPs synthesized by citrate reduction cannot be isolated from the solution since the citrate ions are only weakly adsorbed on the gold surface. In comparison, thiolates (RS<sup>-</sup>) can form a strong covalent bond to the gold core, since both gold and sulphur are considered to be 'soft'.<sup>50</sup> Therefore, thiolate protected AuNPs are much more stable. The breakthrough method reported<sup>51-53</sup> by Brust and Schiffrin *et al.* is a

convenient method to synthesize stable and isolable AuNPs. This is a biphasic method, in which tetraoctylammonium bromide ( $(C_8H_{15})_4N^+Br^-$ ) acts as a phase transfer agent to transport chloroaurate and the reducing agent ( $BH_4^-$ ) to the organic phase. Au(III) is then mixed with the hydrophobic protecting ligand (*e.g.* thiol) and reduced with borohydride (Scheme 2.2).



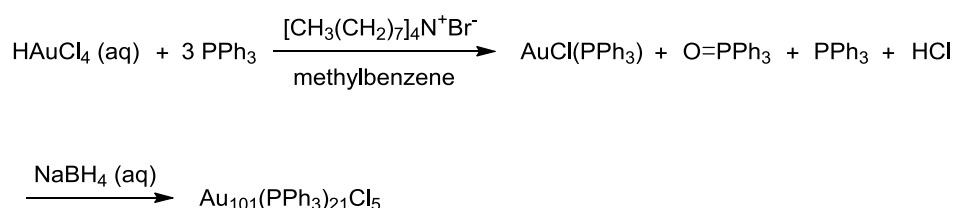
**Scheme 2. 2. Brust-Schiffrin synthesis of AuNPs.**

The AuNPs synthesized by the biphasic method are protected by hydrophobic thiolate ligand via strong covalent bonding, thus can be isolated and redispersed in appropriate hydrophobic solvents. In the particle formation process, naked gold cores formed from reduction of Au(III) are immediately surrounded by the self-assembled monolayers (SAMs), namely the thiolate ligands. The Brust-Schiffrin method is widely adopted to synthesize stable monolayer-protected clusters (MPCs) due to its convenience and simplicity, and has had a significant impact on the advances of nanotechnology.

### 2.1.3.3. AuNPs protected by phosphanes

In Faraday's early study<sup>9</sup> of colloidal gold, phosphorus was the reagent used for reduction of Au(III). In fact, the Au-P bond is rather strong (although not as strong as Au-S bond) which makes phosphanes excellent stabilizers for AuNPs. Schmid reported his well-known  $Au_{55}(PPh_3)_{12}Cl_6$  cluster in 1981<sup>54</sup>, formed by reduction of gold salt with gaseous  $B_2H_6$  in the presence of triphenylphosphine. Hutchison *et al.*<sup>55</sup>

improved the synthesis of PPh<sub>3</sub> protected AuNPs by adopting the Brust biphasic method. In Hutchison's modification, HAuCl<sub>4</sub> was transferred from aqueous to organic phase in the presence of a phase transfer agent (*e.g.* (C<sub>8</sub>H<sub>15</sub>)<sub>4</sub>N<sup>+</sup>Br<sup>-</sup>) and then reduced by NaBH<sub>4</sub> (Scheme 2.3). By replacing the diborane reductant with borohydride, this method allows synthesis of a larger quantity of AuNPs, which increases the tolerance to various phosphine ligands. The biphasic method results in small AuNPs with the size *ca.* 1.5 nm.



**Scheme 2. 3. Biphasic synthesis of PPh<sub>3</sub> protected AuNPs.**

#### 2.1.4. Particle size control

Size control is crucial for engineering AuNPs due to the importance of many size-dependent properties (*e.g.* cytotoxicity). There are generally two ways to control the size of the AuNPs, by adjusting synthetic conditions and post-synthesis modifications.

##### 2.1.4.1. Size control by adjusting synthetic conditions

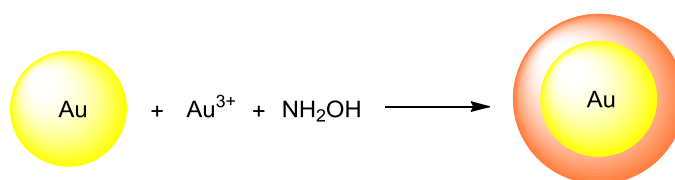
In the synthesis of thiolate protected AuNPs, particle size can be controlled by adjusting the concentration of thiol and gold salt. Increasing thiol to gold ratio leads to smaller particles. The size of AuNPs made by this method typically ranges from 2 to 5 nm and is narrowly dispersed.

Similarly, the size of AuNPs synthesized from the citrate reduction method can also be tuned by varying the reaction conditions (*e.g.* concentrations of the reagents and pH), AuNPs can be synthesized in the size ranging from 14 to 900 nm.<sup>12</sup>

### 2.1.4.2. Post-synthesis modification

#### *Seeding growth*

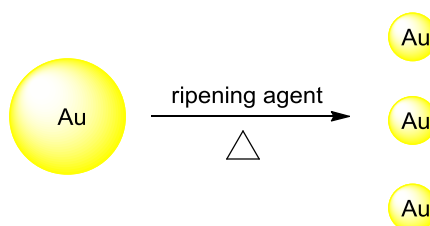
Seeding growth<sup>56-59</sup> of citrate ion protected AuNPs results in size enlargement and increasing monodispersity. Typically, seed AuNPs (*e.g.* synthesized by citrate reduction) were immersed into a solution of Au(III) and hydroxylamine (*e.g.* NH<sub>2</sub>OH). Reduction of Au(III) by NH<sub>2</sub>OH is catalyzed by the surface of seed particles, therefore leading to growth of AuNPs but not new particle nucleation (Scheme 2.4).



**Scheme 2. 4. Hydroxylamine seeding growth of AuNPs.**

#### *Digestive-Ripening*

Digestive-ripening treatment has also been demonstrated<sup>60-62</sup> to control the size, shape and size distribution of AuNPs. Typically, colloidal gold is heated in the presence of a digestive-ripening agent (*e.g.* alkanethiol), leading to reduced average particle size and increased monodispersity (Scheme 2.5). The resulting AuNPs are also functionalized with thiolate ligands and thus can be isolated and re-dissolved in non-polar solvents.



**Scheme 2. 5. Digestive-ripening of AuNPs.**

### 2.1.4.3. Structure and morphology of AuNPs

Despite the extensive studies of AuNPs, the conformation of the ligand shell as well as the gold core has long been obscure. Many studies were based on an idealized model in which a spherical gold core is surrounded by the thiol ligands attached to it. In this thesis, AuNPs are also shown in this conventional way due to its simplicity. Since AuNPs are almost never pure and monodisperse, they are often described as an average of the components. Thus, AuNPs are often represented by the number of gold atoms and ligands, calculated from the average particle diameter and composition. Recently published crystal structures of thiol coated AuNPs is thus a key step forward which leaves no ambiguity about their structure. The structure<sup>63</sup> (Figure 2.1) of a  $\text{Au}_{102}$  particle has a centrosymmetric space group  $C2/c$ . The 49-atom Au core packed in a Marks decahedron with two 20-atom caps at both poles. There are also 13 Au atoms scattering on the equator with no apparent symmetry.

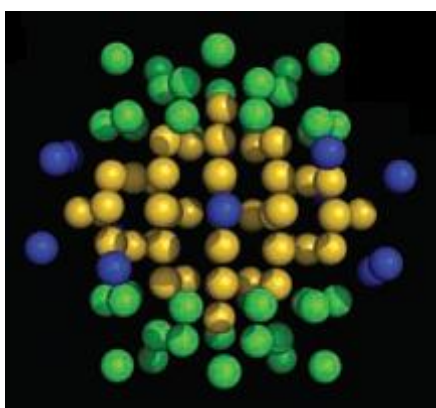


**Figure 2. 1. Crystal structure of  $\text{Au}_{102}(\text{pSC}_6\text{H}_4\text{COOH})_{44}$ . Yellow: Marks decahedron core. Green: the two 20-atom caps at the poles. Blue: the 13-atom equatorial band.**

A later reported<sup>64</sup> structure of  $[\text{N}(\text{C}_8\text{H}_{17})_4][\text{Au}_{25}(\text{SCH}_2\text{CH}_2\text{C}_6\text{H}_5)_{18}]$  has a 13-atom icosahedron core with another 12 Au atoms stellating on 12 of the 20 faces (Figure 2.2). The outer 12 gold atoms are networked via thiolate ligands.

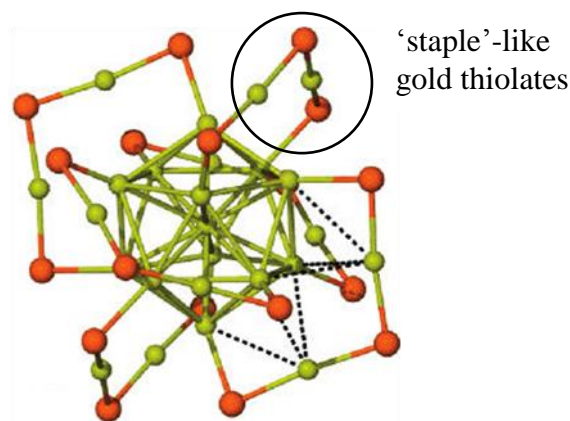


**Figure 2. 2. Crystal structure of  $[N(C_8H_{17})_4][Au_{25}(SCH_2CH_2C_6H_5)_{18}]$ . Yellow: gold. Orange: sulphur.**

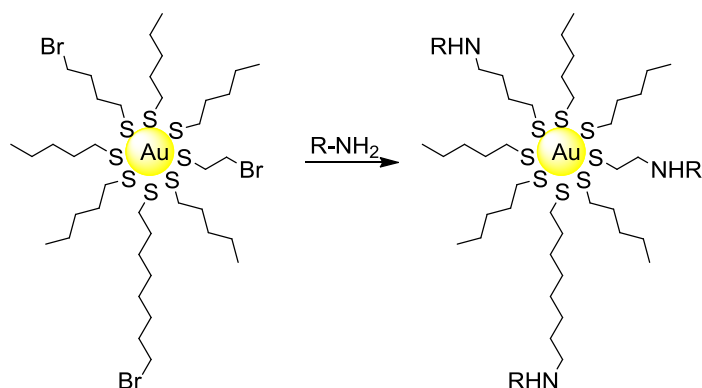
Interestingly, in the reported crystal structures, classically defined vertex and edge sites are not unambiguously identified. Non-equivalence of the surface sites suggests that AuNPs are chiral. The arrangement of gold atoms in Au core is very similar to bulk gold. The Au core is surrounded not by thiol ligands, but by gold thiolate ‘staples’ (as highlighted in Figure 2.2). The AuNPs are stabilized by both Au-S bonding and interactions between the ligand molecules, which supports the tight packing of ligand shell.

#### 2.1.4.4. Functionalization of AuNPs

Applications of AuNPs in bio-medical area and catalysis<sup>65</sup> require functionalization of the metal surface. Various methods have been developed to introduce functional groups to AuNPs.

##### *Reactions of the end group of the stabilizing ligand*

Conventional organic chemistry reactions can be applied<sup>66-67</sup> to the end group of the protecting ligand on AuNPs (Scheme 2.6). For instance, coupling of the carboxylate groups at the free ends of the stabilizing ligands of AuNPs to the amino groups in biological molecules is an important way to introduce bio-functionalization<sup>68</sup>.



**Scheme 2. 6. Reaction of  $\omega$ -bromo-functionalized AuNPs with primary amines.**

### *Ligand exchange reaction*

The ligand exchange reaction reported<sup>69</sup> by Murray and co-workers is an extremely useful tool in functionalization of AuNPs. For instance, thiolate ligands on the AuNPs surface can be replaced by another thiol ligand (Scheme 2.7).



**Scheme 2. 7. Ligand exchange reaction of thiolate protected AuNPs.**

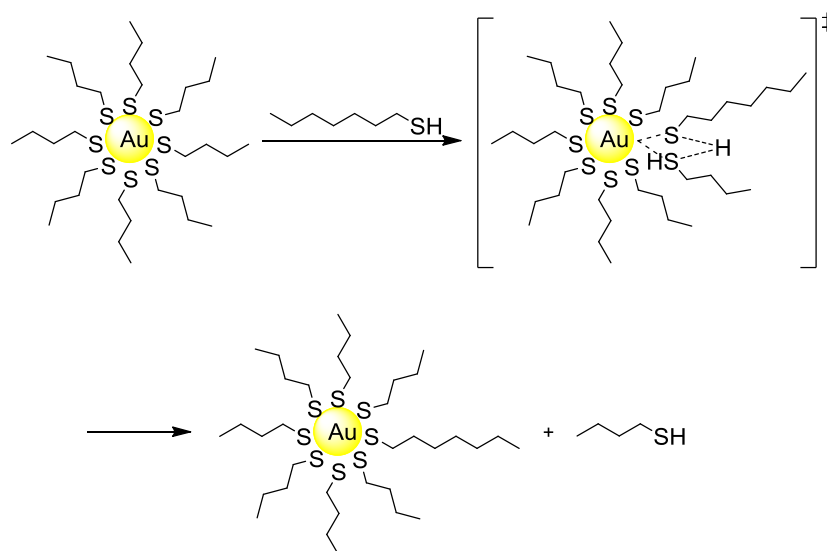
Murray *et al.* demonstrated that poly homo-<sup>70</sup> and poly hetero-<sup>71</sup>functionalized AuNPs could be obtained using the exchange reaction.

#### **2.1.4.5. Mechanism of ligand exchange reaction**

Ligand exchange reaction makes it possible to functionalize AuNPs. This method not only provides a means to introduce ligands which are incompatible with the synthetic conditions, but also to engineer nanoparticle-based devices with different functionalities. Due to the importance of this reaction, the reaction mechanism was studied by many researchers. As the results showed, the chemistry of ligand exchange is complicated.

*Ligand exchange reaction of thiolate protected AuNPs with thiols*

Thiolate ligand stabilized AuNPs undergo ligand exchange reaction with thiols via an associative ( $S_N2$ -type) mechanism<sup>69, 71-73</sup>, yielding a new thiol (Scheme 2.8). The exchange is a dynamic equilibrium. Disulfide products were not reported to be involved in the ligand exchange.



**Scheme 2. 8. Mechanism of ligand exchange reaction of thiols with thiolate protected AuNPs.**

The rate and extent of ligand exchange depend on both incoming and outgoing ligands. Generally, thiols with longer chain length readily replace short chain thiolates on the AuNPs surface. Long chain thiol coated AuNPs are more stable, since the packing of SAM on the gold core is tighter, thus providing better protection. The reaction rate of cyanide (i.e.  $CN^-$ ) induced AuNP decomposition decreases with increasing chain length of the protecting thiolate ligand<sup>74</sup>, which confirms the ‘solid-like’ packing of long chain SAMs on the gold surface. Furthermore, the extent of ligand exchange also depends on the chain length of the protecting ligand<sup>71</sup>. Many more ligands can be replaced from short chain SAMs.

Different sites on the AuNPs surface are considered to have different reactivity in ligand exchange reaction. In the studies of exchange reaction on monolayer protected gold particles, particularly in 2-D SAMs (*e.g.* flat Au surface), reports<sup>75-76</sup> have shown that some sites are significantly more reactive than others. Murray and co-

workers<sup>72</sup> then interpreted this observation and concluded that ligand exchange reaction starts from certain surface sites (*e.g.* classically defined vertex and edge sites). Other sites (*e.g.* terrace sites) react much slower therefore can only be observed at the later stage of ligand exchange. A later study<sup>73</sup> by the same group also suggested that the rate of exchange does not depend on particle size, which supports the hypothesis that certain surface sites are primarily targeted in the initial ligand exchange reaction. However, in the recently reported crystal structures of AuNPs, well defined defect sites in the classic geometric models were not observed. Therefore, the different reactivity of the binding sites is unlikely to be simply related to geometric features.

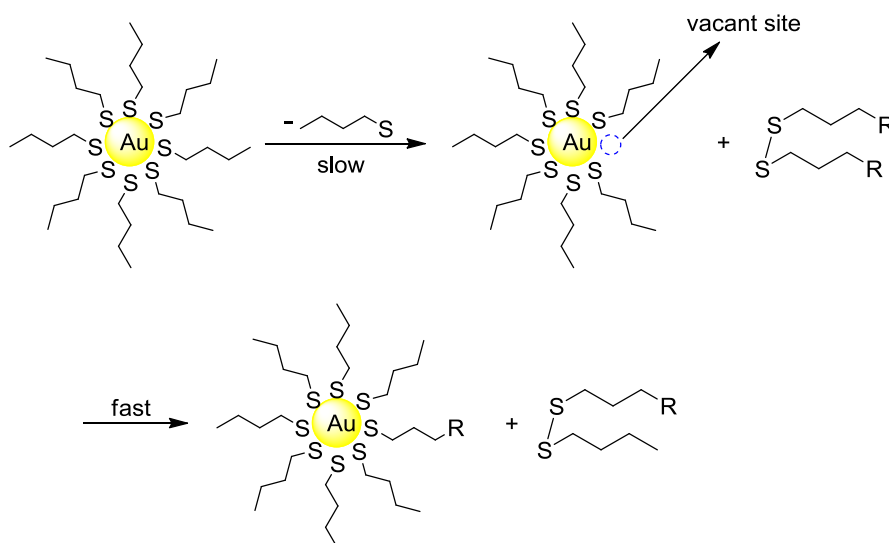
#### *Ligand exchange reaction of PPh<sub>3</sub> protected AuNPs with thiols*

The phosphorus-gold bond is not as strong as the sulphur-gold bond, therefore triphenylphosphine protected AuNPs can be considered to have a ‘looser’ shell than thiolate coated AuNPs. In the ligand exchange reaction, the PPh<sub>3</sub> SAM is much more exchangeable than thiolate. For PPh<sub>3</sub> protected AuNPs<sup>77-78</sup>, in addition to significantly faster reaction rate, almost all phosphine ligands can be replaced by thiolate ligands in the exchange. This property makes PPh<sub>3</sub> AuNPs an important precursor in functionalization of nanoparticles.

#### *Ligand exchange reaction of thiolate protected AuNPs with disulfides*

Disulfides are much less reactive than thiols in the ligand exchange reaction. Studies of ligand exchange reaction of disulfide on 2-D SAM suggested that S-S bond cleaves during exchange<sup>79</sup>, and the reaction was slow. The ligand exchange reaction of thiolate protected AuNPs with disulfides was found<sup>80-81</sup> to follow a dissociative (S<sub>N</sub>1 type) mechanism (Scheme 2.9), in which desorption of the outgoing ligand is the rate determining step. After dissociation of thiolate ligand, the vacant site on the gold surface can attack the S-S bond of disulfide, leading to cleavage of the disulfide bond. Interestingly, the two thiolate branches do not attach to the gold surface on sites adjacent to each other. This observation suggests that the exchange of the two thiolate branches is stepwise. The extent of ligand exchange of AuNPs with

disulfides was found to be much smaller than thiols, which indicates different reaction mechanisms.



**Scheme 2. 9. Mechanism of ligand exchange reaction of disulfides with thiolate protected AuNPs**

#### *Reaction intermediates in ligand exchange reactions*

Gold thiolates were suggested to be possible intermediates in the ligand exchange reactions. Particularly, Murray and co-workers observed<sup>82</sup> both ligand exchange and metal transfer in inter-particle exchange. This observation is consistent with the involvement of gold thiolates (*e.g.* Au-SR) as reaction intermediate in ligand exchange. The kinetics of inter-particle ligand exchange suggests a dissociative reaction pathway<sup>83</sup>. One can imagine that ligand dissociation from the gold surface may not only be in the form of free ligand, but also as gold thiolate. Furthermore, in studies of ligand exchange of thiolate and PPh<sub>3</sub> protected AuNP, loss of Au atoms from the particle was observed. Although the difference is far from significant to cause a noticeable size change, the observation also indicates possible involvement of oxidized gold in the reaction mechanism. In the recently reported crystal structures of AuNPs, gold thiolates ‘staples’ were found surrounding the Au core, which supports involvement of gold thiolates in exchange reactions.

Thiolate radical intermediates were found<sup>84-85</sup> in the ligand exchange of PPh<sub>3</sub> coated AuNPs with thiols in the presence of oxygen. The amount of radicals involved was found to be large, therefore radical mechanism is likely to be a major reaction pathway for the ligand exchange of PPh<sub>3</sub> AuNPs. The important role of oxygen also indicates catalytical oxidation of thiols by O<sub>2</sub>. Oxidation of thiols leads to loss of the sulphur-bound H atoms and formation of thiolate radicals. The fate of the H atoms during SAM formation<sup>86</sup>, however, remains unclear. In comparison, no radicals were detected in the ligand exchange of thiolate stabilized AuNPs with thiols.

#### 2.1.4.6. Packing, migration and dynamics of the ligands on AuNPs

Murray *et al.* suggested<sup>71</sup> that short chain, bulky alkanethiols are the least thermodynamically stable ligands hence tend to be displaced by thiols with longer chain. As discussed in Section 2.1.4.5 (p36), short chain thiolate protected AuNPs react faster and long chain coatings are favourable in the equilibrium of exchange. Indeed, the appreciable difference in reaction rate and the position of equilibrium in ligand exchange leads to the suggestion that short chain alkanethiols are less stable as stabilizing agents. The implication behind these observations is that the packing of SAM on the gold surface is tight, thus long chain thiols form a tighter shell on the AuNPs and provide better protection.

Since different sites exist on the AuNPs, it was suggested<sup>72</sup> that ligand could migrate on the gold surface between different sites. The loss of Au atoms and potential gold thiolate intermediates during ligand exchange are also consistent with the surface migration scenario. However, a lack of lateral diffusion<sup>87</sup> of the thiolate ligand on Au surface suggests that ligand migration is more likely to be a very slow process, possibly associated with inter-particle gold thiolate exchange.

Tumbling of the protecting ligand is slow due to attachment to the gold surface. NMR spectra of the end group of the thiolate ligand are broader<sup>71</sup>. In particular, no signal can be detected for the CH<sub>2</sub>S group in the NMR spectroscopy due to long relaxation time. Similarly, EPR spectra of AuNPs spin labelled with a stable free

radical functionalized thiolate ligand also suggest slower tumbling rate as compared to the free label (Figure 2.3).

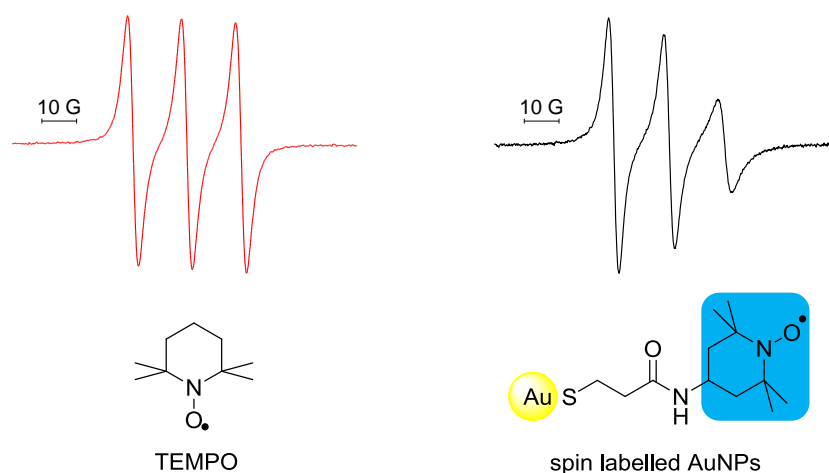


**Figure 2. 3. EPR spectra of TEMPO and C<sub>4</sub>S-AuNPs spin labelled with a nitroxide radical.**

In addition, the mobility of the spin label varies with the chain length of the protecting ligand<sup>88</sup>. For instance, EPR spectrum of AuNPs with a thick ligand shell (*e.g.* coated by long chain thiols) carrying a short chain spin label falls to the slow motion regime. It confirms that the surroundings (*e.g.* ligand shell) of the spin-label are more ‘solid like’ rather than ‘liquid like’.

#### 2.1.4.7. Ageing of AuNPs

An early study by our group found that ageing of AuNPs in solution strongly affected the rate of the ligand exchange reaction of AuNPs with disulfides<sup>89</sup>. The reactivity of AuNPs in place-exchange with disulfides is dramatically reduced by ageing in solution at room temperature. Freshly synthesized AuNPs were found to react nearly 10 times faster than aged particles. No appreciable size change was observed during ageing. The preliminary observation is interesting, however, the origin and scope of this effect remains unclear. The ageing effect may be attributed to ageing of SAM or ageing of gold core. The effect could be only on the reaction rate or on the number of exchangeable sites as well.

### **2.1.5. Aim and objectives**

Significant efforts have been made to explore the physics and chemistry of AuNPs. And indeed, an adequate understanding was achieved for the current applications of nanoscience. However, as the field develops, the understanding of many aspects of nanomaterials need to be strengthened, more detailed functionalization mechanism need to be addressed to precisely engineer nanoscale or even sub-nanoscale devices. In this context, a better understanding of reactivity and mechanism of ligand exchange may be achieved in this chapter. Ageing of AuNPs was observed by our group but the effect was not studied in detail. The investigation of ageing effect of AuNPs helps to understand different binding sites on the Au surface which is important in the catalytical applications of AuNPs. Understanding the reactivity of fresh and aged AuNPs is useful in engineering nanoparticle-based devices. Hence, the aim of this chapter is to understand the mechanistic features of ageing effect of AuNPs, including the origin and scope of such effect. Through possible underlying implications of the ageing effect, light could be shed on some obscure aspects of ligand exchange and different binding sites on AuNPs.

This chapter describes the reactivity of fresh and aged thiolate stabilized AuNPs towards disulfide exchange. The ligand and temperature dependence of ageing and the effect of ageing on the equilibrium position of ligand exchange allowed us to understand the mechanism of the ageing process and gave some understanding on the structure of the AuNPs surface.

## **2.2. Investigation methodology**

### **2.2.1. Target AuNPs**

Citrate, thiolate and triphenylphosphine coated AuNPs are the dominant precursors in the functionalization of nano sized devices. Citrate ion stabilized AuNPs are protected by electrostatic repulsion and are not isolable or redispersible. PPh<sub>3</sub> coated AuNPs are very reactive, thus are very useful in functionalization. However, they are

less stable than thiolate coated AuNPs. And more importantly, PPh<sub>3</sub> protected AuNPs were found to be batch dependent in terms of reactivity. The reproducibility of PPh<sub>3</sub> coated AuNPs seems to rely on the easily overlooked details during the synthetic process which are difficult to control. Thiolate protected AuNPs, in contrast, are isolable and more stable. Their ligand exchange reaction is slower therefore is convenient to monitor. Hence, ageing of thiolate stabilized AuNPs was targeted in this investigation.

The reaction of AuNPs with disulfides appears to be simpler than thiols, which makes it a good model to understand certain aspects of the ligand exchange (*e.g.* reactive sites *etc.*). In addition, unpublished results from our group show that in ligand exchange of AuNPs with thiols, such significant ageing effect was not observed. Thus, the reaction mechanism of AuNPs with disulfide and thiols could be differentiated. As a result, the ligand exchange of thiolate protected AuNPs with disulfide was chosen as a model system in this chapter.

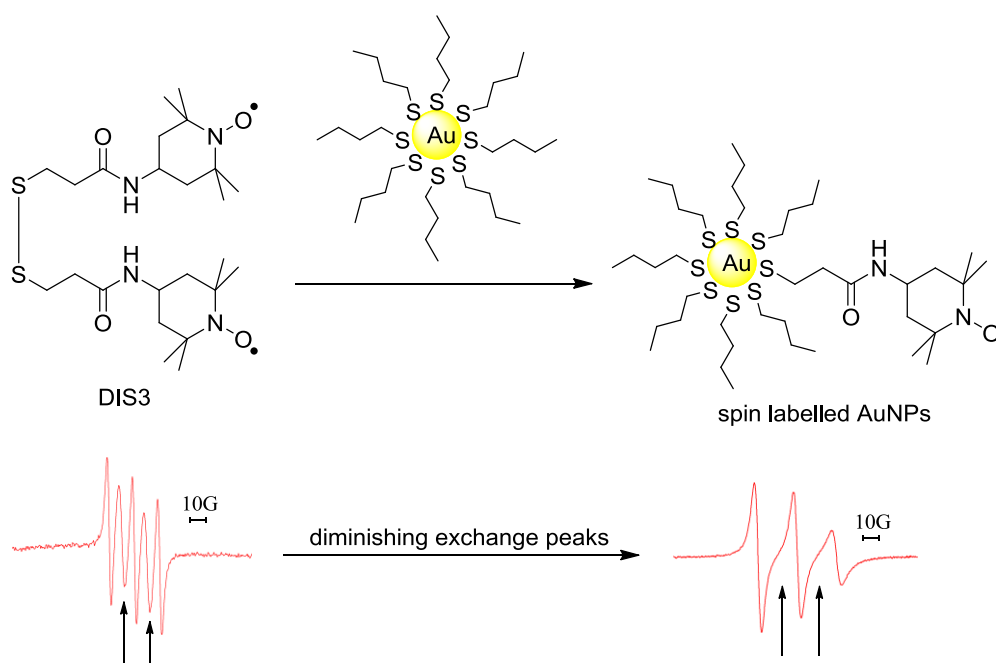
### 2.2.2. Analytical method survey

Ligand exchange reactions were mostly studied by NMR and FT-IR spectroscopy as firstly demonstrated<sup>71</sup> by Murray and co-workers. In their studies, NMR spectroscopy was employed to monitor nanoparticle formation, structure and stoichiometry. FT-IR spectroscopy was used to study surface disorder. Their studies target the reaction of AuNPs with thiols, where the extent of exchange is significant. However, their methodology cannot be applied in our investigations due to the small amount of reacted disulfide and associated products. Other spectroscopic methods were also reported to be used in the investigations of ligand exchange reactions, including fluorescence<sup>90</sup> and EPR spectroscopy<sup>80-81</sup>. These two methods are similar in many ways. They are both sensitive, they both involve labelling of the AuNPs with appropriate functional groups, and they both can monitor ligand exchange *in situ*. The advantage of EPR spectroscopy in this investigation is that it is possible to obtain information on ligand dynamics on AuNPs. Taking into account that this technique was used in our group to investigate this very topic and the methodology

was already developed, EPR spectroscopy was chosen as a major analytical tool in this study.

### 2.2.3. Model system

In order to monitor the ligand exchange reaction with EPR spectroscopy, a customized bisnitroxide disulfide, 'DIS3', was employed. The compound was synthesized via coupling of amino-TEMPO with the corresponding disulfide precursor by lab colleagues. This disulfide contains two spin labelled branches which gives a five-line EPR spectrum due to exchange interactions. The disulfide ligand itself is stable at 90 °C in a chlorobenzene solution, as the EPR spectrum of 'DIS3' does not change over time. When reacting with gold nanoparticles, the S-S bridge cleaves and one branch attaches to gold surface to form spin labelled nanoparticle which give a three line EPR spectrum. The height of exchange peaks (highlighted with arrows in Scheme 2.10) is proportional to DIS3 concentration.



**Scheme 2. 10. Ligand exchange reaction of AuNPs with bisnitroxide disulfide DIS3. The exchange peaks of DIS3 diminishes during reaction.**

## 2.3. General synthesis and characterization of AuNPs

### 2.3.1. Typical synthesis protocol

AuNPs were prepared by the Brust two-phase protocol. Typically, hydrogen tetrachloroaurate trihydrate ( $\text{HAuCl}_4 \cdot 3\text{H}_2\text{O}$ ) was dissolved in deionised water to make a 1% w/w solution. The  $\text{HAuCl}_4$  (aq) solution was then mixed with tetraoctylammonium bromide (TOAB) and methylbenzene under stirring. Visually, the colour of the aqueous phase turned from yellow to colourless, while the colour of the methylbenzene phase became red-brown. This suggests Au(III) was transferred to the organic phase. A 10% w/w solution of alkanethiol in methylbenzene was then added to the reaction mixture. Immediately afterwards (*e.g.* in 20s), an aqueous solution of  $\text{NaBH}_4$  was added under vigorous stirring. Au(III) was reduced to Au(0) within seconds, which can be observed by the colour change of the organic phase to black. In order to minimize ageing, the reaction time was limited to 3 minutes, and the organic phase was separated thereafter. Solvent was evaporated and the crude particles were washed with methanol and eventually dried under  $\text{N}_2$  flow. The entire preparation typically takes *ca.* one hour hence guarantees the freshness of AuNPs. Product was dark powder, and has a typical yield of 75%.

### 2.3.2. Characterization of AuNPs

AuNPs synthesized in this investigation were characterized using a series of analytical methods. For instance, the characterization of *n*-butanethiol protected AuNPs (represented as  $\text{C}_4\text{H}_9\text{S}$  AuNPs in this chapter) is demonstrated here (Figure 2.4). Transmission electron microscopy (TEM) revealed the average particle diameter was 1.3nm. The UV-*vis* spectrum of the particles showed a weak plasmon band which is consistent with the small particle size. Thermogravimetric analysis (TGA) curve suggested the thermal decomposition temperature is at about 200 °C and gave a mass ratio of 14% organic content to 86% gold core. Elemental analysis found: 7.119% C, 1.187% H and -0.186% N. The negative nitrogen content is probably due to an artifact of the analysis procedure and was thus neglected. If the composition of the organic content (TGA found 14%) is assumed to be  $(\text{C}_4\text{H}_9\text{S})_n$ , the

mass percentage should be 7.55% C and 1.42% H, which is consistent with the CHN analysis.

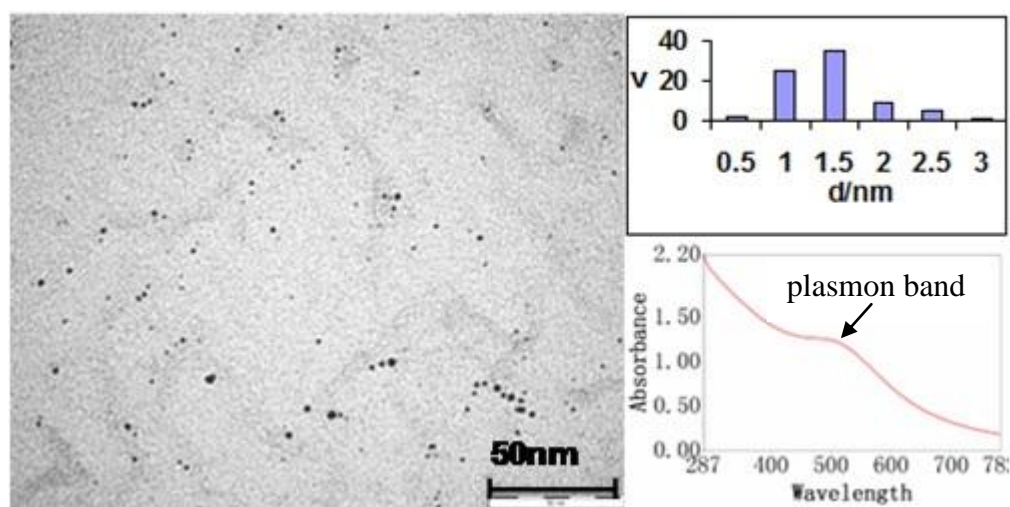


Figure 2. 4. TEM image, particle size distribution and UV spectrum of *n*-butanethiol protected AuNPs.

## 2.4. Reduced reactivity of aged AuNPs

### 2.4.1. Reaction Order

Our group has previously reported that thiolate protected AuNPs react with disulfide via an  $S_N1$  type mechanism<sup>80-81</sup>. A more recent study<sup>91</sup> suggests that ligand exchange can be described by a diffusion limited process. The authors showed that ligand exchange of *n*-decanethiol coated AuNPs ( $C_{10}S$ -AuNPs) with *n*-dodecanethiol ( $C_{12}SH$ ) followed 2<sup>nd</sup>-order diffusion limited Langmuir model (Equation 2.1).

$$\theta(t) = A \frac{k\sqrt{t}}{1+k\sqrt{t}} \quad (2.1)$$

Here,  $\theta$  is the fractional surface coverage of the incoming thiol,  $A$  is the final fractional coverage, and  $k$  is the rate constant.

The concept of the 1<sup>st</sup> and 2<sup>nd</sup> order diffusion limited Langmuir models<sup>92-94</sup> was borrowed from research on micelle kinetics. The diffusion from micelles to binding sites is slow. Although the underlying assumptions of the Langmuir kinetic model make it more suitable for 2-D gold surfaces rather than ligand exchange of AuNPs<sup>95</sup>, we felt it was necessary to re-examine the kinetic profiles based on such diffusion limited models.

#### 2.4.1.1. General data collection and treatment procedure

Ligand exchange reaction of *n*-butanethiol protected AuNPs (C<sub>4</sub>S-AuNPs) with the bisnitroxide disulfide 'DIS3' was therefore monitored by EPR spectroscopy as illustrated in Scheme 2.10. Typically ligand exchange reactions were carried out with chlorobenzene solutions of 10<sup>-4</sup> M AuNPs and 5×10<sup>-5</sup> M DIS3 at different ratios. The ratio described in this chapter refers to the ratio of a nanoparticle to a thiolate ligand. Since one molecule of DIS3 has two thiolate braches, the ratio described as 1:1 means AuNP/DIS3 molar ratio of 2:1. For instance, typically 100 μL 10<sup>-4</sup> M AuNPs reacting with 100 μL 5×10<sup>-5</sup> M DIS3 is described as ratio 1:1. This concept was used because it gives immediate reference to the number of ligands per particle.

To monitor the process of ligand exchange reaction, EPR spectra of the reaction mixture were recorded using a specially written automation program. The program allows automatic multiple EPR measurements with a user-defined time interval (typically 5-10 minute interval was used in this study). As the reaction proceeded, the second and forth peak of the EPR spectra diminished due to consumption of the biradical. Meanwhile, the first, third and fifth peak increased as the total radical concentration stayed the same.

The series of spectra was treated with a spreadsheet in which a Macro was implanted to allow automatic measurements of the peak height within a user-defined field range. The height of the second or the forth peak is proportional to the concentration of the biradical. The time evolution of biradical concentration was used to calculate kinetic parameters for the reaction. The kinetic profiles were thus obtained.

### 2.4.1.2. Ligand exchange of C<sub>4</sub>S-AuNPs: reaction order

Using this protocol, we obtained kinetic profile for ligand exchange of C<sub>4</sub>S-AuNPs and DIS3 with a ratio of 1:1. The kinetic data were fit to a number of kinetic models. The 1<sup>st</sup> and 2<sup>nd</sup> reaction models describe straightforward mono- and bimolecular processes. In the diffusion limited Langmuir models, first order rate of adsorption is scaled by the coverage of available binding sites (1- $\theta$ ). For second order, the rate depends on the incoming ligand and outgoing ligand, both of which scale as (1- $\theta$ ). Therefore the rate is scaled as (1- $\theta$ )<sup>2</sup>.

Fitting of the kinetic profile to the standard 1<sup>st</sup> order model yielded satisfactory result (Figure 2.5). This is consistent with the previous observations.

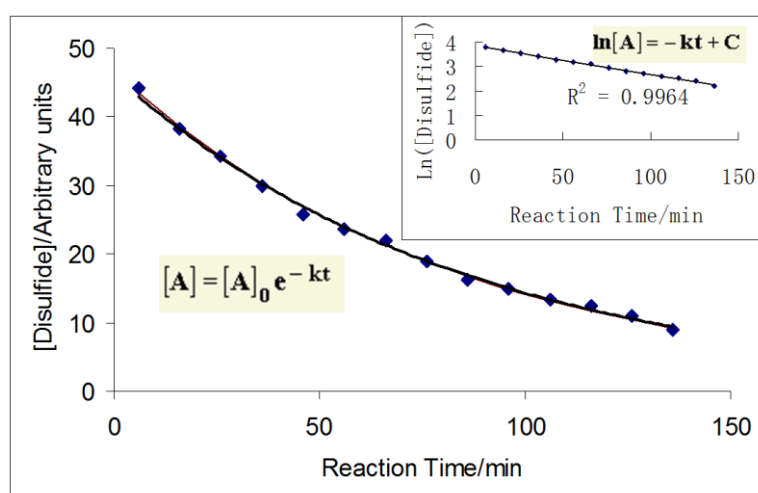


**Figure 2. 5. Fitting of kinetic profile to 1<sup>st</sup> order kinetic model. Solid points are from measured EPR spectra. Black line is simulated result from 1<sup>st</sup> order kinetic model.**

Alternatively kinetic models, including standard 2<sup>nd</sup> order, Langmuir 1<sup>st</sup> and 2<sup>nd</sup> order models resulted in poorer quality fits (Figure 2.6). In fact, the fitting of experimental data to standard 2<sup>nd</sup> order and Langmuir 1<sup>st</sup> order diffusion limited model are not bad. However, by comparison, it is evident that the reaction fits best a standard 1<sup>st</sup> order model.

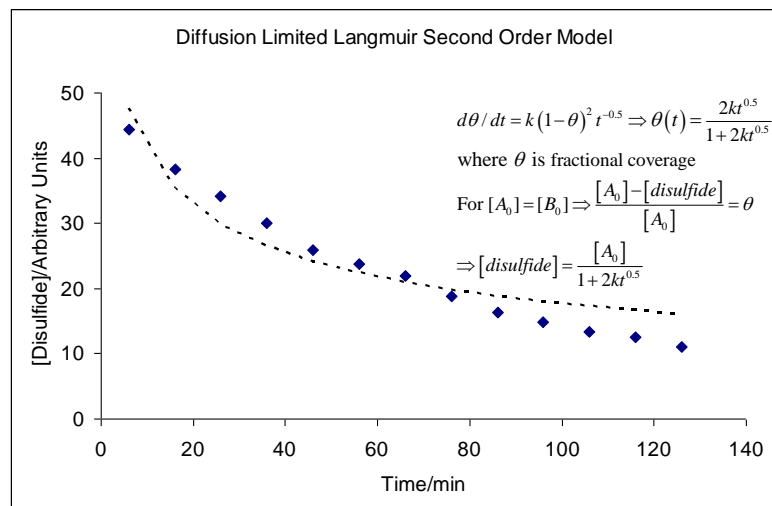
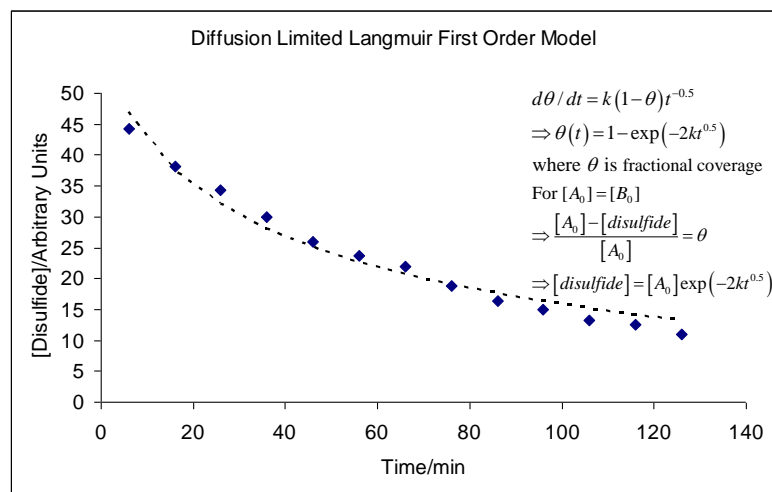
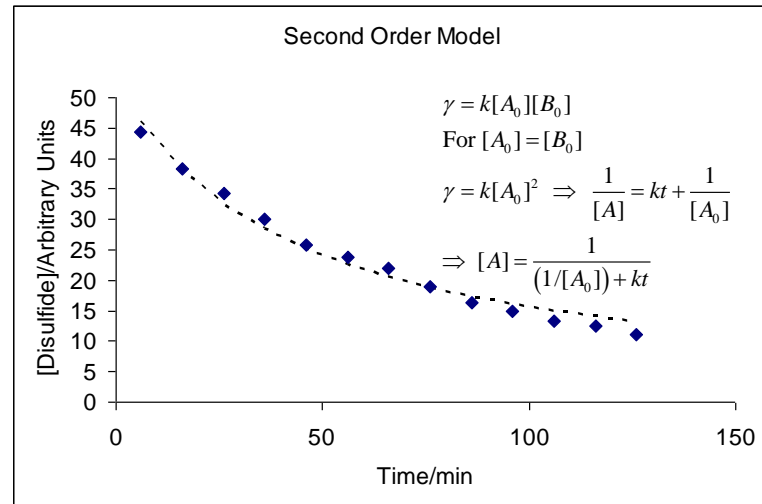


**Figure 2. 6. Unsuccessful fitting of experimental data to standard 2<sup>nd</sup> order model, 1<sup>st</sup> order diffusion limited Langmuir model and 2<sup>nd</sup> order diffusion limited Langmuir model. Solid points are experimental data. Dashed lines are simulated results from the kinetic models.**

### 2.4.1.3. Ligand exchange of C<sub>8</sub>S- and C<sub>18</sub>S-AuNPs: reaction order

It is possible that the differences between our and the reported<sup>91</sup> system might have led to different reaction mechanism. For instance, in the literature ligand exchange was carried out using a long chain thiolate (C<sub>10</sub>S) protected AuNPs, while in our reaction C<sub>4</sub>S-AuNPs were used. Since ligand packing on the nanoparticle surface is tight, thicker ligand shell could affect the accessibility of certain reactive sites. If such scenario is true, diffusion of incoming ligand from the ligand shell to Au surface may be a slow step thus determining the overall reaction rate. To clarify such ambiguities, kinetic data of ligand exchange of C<sub>8</sub>S-AuNPs and C<sub>18</sub>S-AuNPs with DIS3 were also analyzed in a similar way.

Similarly, the biphasic method was used to prepare *n*-octanethiol protected AuNPs (C<sub>8</sub>S-AuNPs). Ligand exchange of C<sub>8</sub>S-AuNPs and DIS3 at room temperature (*e.g.* 20 °C) using a ratio of 1:1 was monitored by EPR spectroscopy. The kinetic data were fit to standard and diffusion limited models, and resulted in reasonable fit to both models (Figure 2.7). However, in comparison, the quality of fitting to standard 1<sup>st</sup> order is appreciably better. It clearly suggests that reaction of C<sub>8</sub>S-AuNPs with DIS3 still follows standard dissociative route.

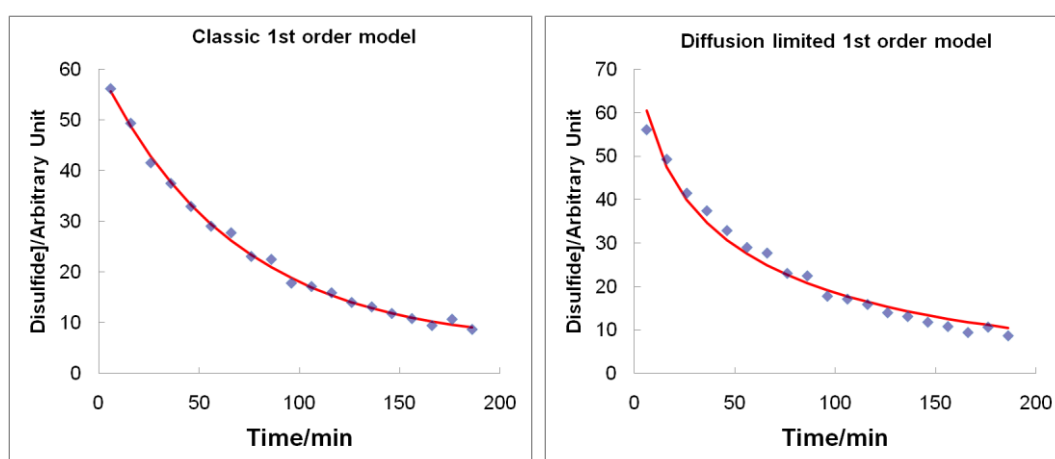


**Figure 2. 7. Kinetic data of reaction of C<sub>8</sub>S-AuNPs with DIS3 and the fitting to standard and diffusion limited 1<sup>st</sup> order model. Solid points: experimental data. Red line: simulation.**

The reaction of *n*-octadecanethiol protected AuNPs (C<sub>18</sub>S-AuNPs) with DIS3 showed similar result. C<sub>18</sub>S-AuNPs were synthesized using a similar method. The

ligand exchange reaction was carried out at room temperature using a 1:1 AuNP/DIS3 ratio. Similarly, kinetic data were fit to a number of kinetic models and the outcome showed standard and diffusion limited 1<sup>st</sup> order models were the most probable models for this reaction (Figure 2.8). We believe that standard 1<sup>st</sup> order still gave a better fit than the diffusion limited model.

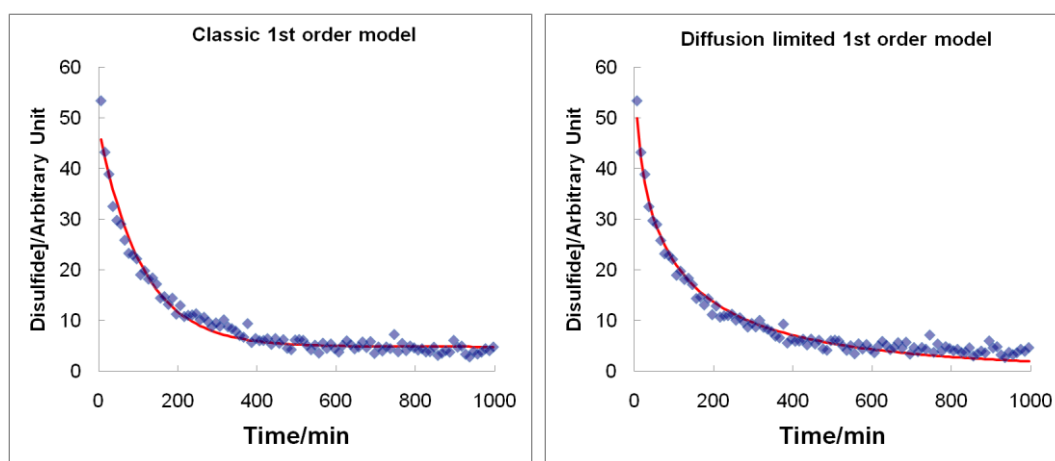


**Figure 2. 8. Kinetic data of reaction of C18S-AuNPs with DIS3 and the fitting to standard and diffusion limited 1<sup>st</sup> order model. Solid points: experimental data. Red line: simulation.**

More importantly, the diffusion limited Langmuir kinetic model assumes that the concentration of the incoming ligand does not change which is only true for the pseudo 1<sup>st</sup> order conditions. Ligand exchange is in fact an equilibrium, however, the reverse reaction is not included in the Langmuir models. Furthermore, diffusion limited kinetic model assumes a low activation energy which is unlikely to be true in ligand exchange reactions. Different incoming ligands with similar steric effects were found to react at appreciably different rates in exchange reactions<sup>96</sup>, which is also against the diffusion limited kinetics.

In summary, kinetic profiles of ligand exchange were re-examined by using AuNPs with different ligand chain length. The outcome suggests that up to C<sub>18</sub>S-AuNPs, the reaction order does not depend on chain length or organic shell thickness. It is noticed that in the original report<sup>91</sup>, the reaction was monitored much longer (10 times) than our investigation. At a later stage, ligand exchange is close to equilibrium and reaction becomes slow. The concentration of the incoming ligand

can thus be considered as constant. Therefore, our results do not necessarily rule out diffusion controlled kinetics at a later stage of ligand exchange.

### **2.4.2. Reduced reactivity of aged AuNPs in ligand exchange reactions**

As the kinetic model for ligand exchange of AuNPs with disulfides was confirmed, ageing effect on AuNPs was studied. AuNPs were synthesized as described in Section 2.3.1 (p45). The synthesis and purification of AuNPs was restricted to *ca.* one hour to minimize ageing. Freshly prepared particles were dried and dissolved in chlorobenzene to make a  $10^{-4}$  M solution. AuNPs were then aged in solution at room temperature (unless stated otherwise). Aliquots (typically 100  $\mu$ L) of the AuNPs solution were taken at different ageing time and mixed with DIS3 solution ( $5 \times 10^{-5}$  M) in an EPR tube using different nanoparticle/thiolate ligand ratio. The sample was then placed into the EPR cavity and the reaction was monitored. During the kinetic study, the sample was not taken out or moved to avoid re-tuning the EPR spectrometer.

#### **2.4.2.1. Ageing effect on C<sub>4</sub>S-AuNPs**

The investigation was started with reproducing our previous observation<sup>89</sup>. Ligand exchange of C<sub>4</sub>S-AuNPs with DIS3 was carried out at room temperature (*e.g.* 20 °C) using a ratio of 1:1 nanoparticle/thiolate branch. A series of EPR spectra were recorded and the kinetic profiles for fresh and aged AuNPs were generated. As discussed in Section 2.4.1 (p46), the kinetic data were fit to a standard 1<sup>st</sup> order model and kinetic parameters were thus obtained. Significant decay of reactivity of aged particles was clearly observed. The reaction rate of fresh C<sub>4</sub>S-AuNPs was almost 10 times as fast as the rate for particles aged for 79h (Figure 2.9). This effect was also proved reproducible.

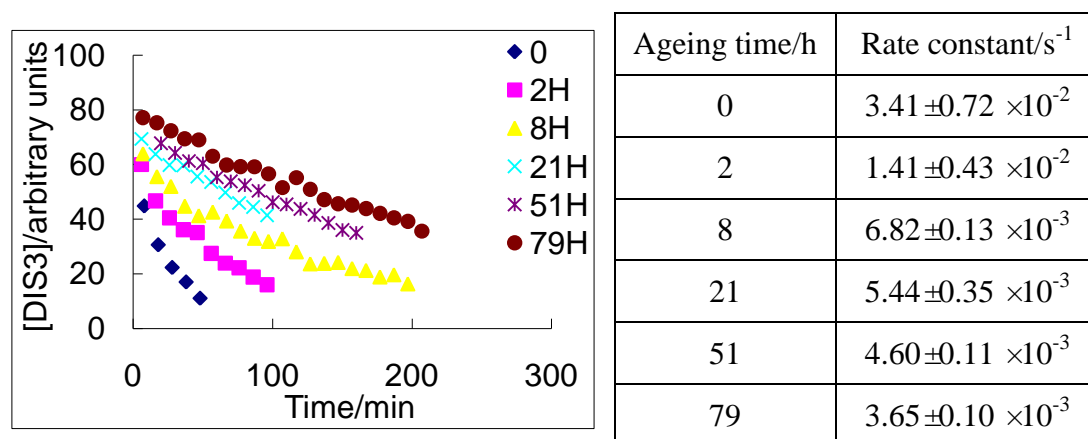
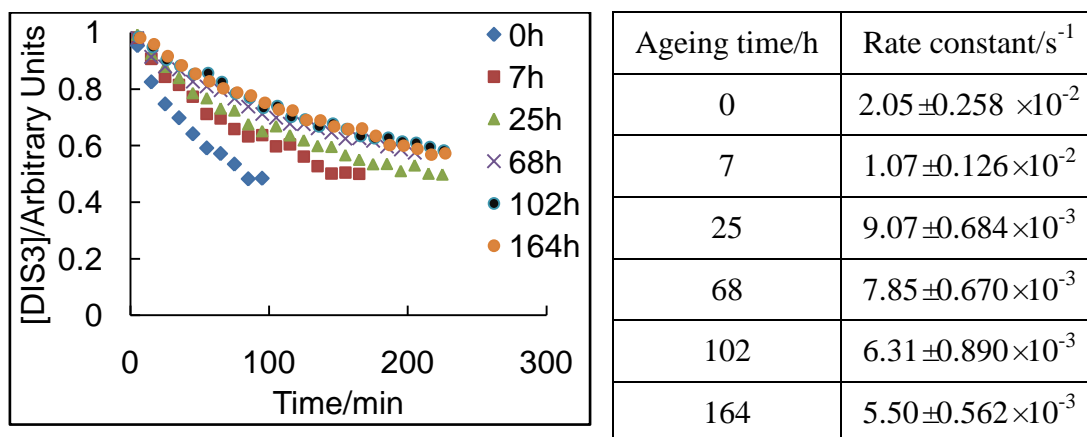


Figure 2. 9. Kinetic profiles and rate constants of ligand exchange reactions of C<sub>4</sub>S-AuNPs and DIS3 with 1:1 ratio, at room temperature.

#### 2.4.2.2. Effect of reaction temperature on ageing effect

If we assume that different sites on the nanoparticle surface have different activation barrier, reaction at an elevated temperature would involve more sites. In order to understand the effect of ageing on different types of sites on AuNPs, the temperature dependence of ageing was studied.

Ligand exchange reaction of a 1:10 C<sub>4</sub>S-AuNP/DIS3 mixture was monitored at 40 °C. This ratio was used to allow maximum extent of exchange on AuNPs. The studies on the extent of ligand exchange are discussed later in Section 2.5 (p64). Due to the presence of excess disulfide, the reaction does not go to completion. The AuNPs aged for 164 h reacted about 4 times slower than the fresh particles (Figure 2.10). Aged particles showed reduced reactivity, however, the effect is not as evident as at room temperature.



**Figure 2. 10. Normalized kinetic profiles and rate constants of ligand exchange reactions of C<sub>4</sub>S-AuNPs and DIS3 with 1:10 ratio, at 40 °C.**

An interesting observation from the ligand exchange at room temperature and 40 °C is the different temperature dependence of the reaction rate of fresh and aged AuNPs. Due to the batch-dependent properties of AuNPs and the effect of ageing, direct comparison of the reaction rate of fresh AuNPs at different temperature is not easy. However, statistically, we found ageing effect is less significant if the reaction is carried out at higher temperature. Figure 2.11 compares the change of reaction rate at different temperature as the AuNPs were aged.

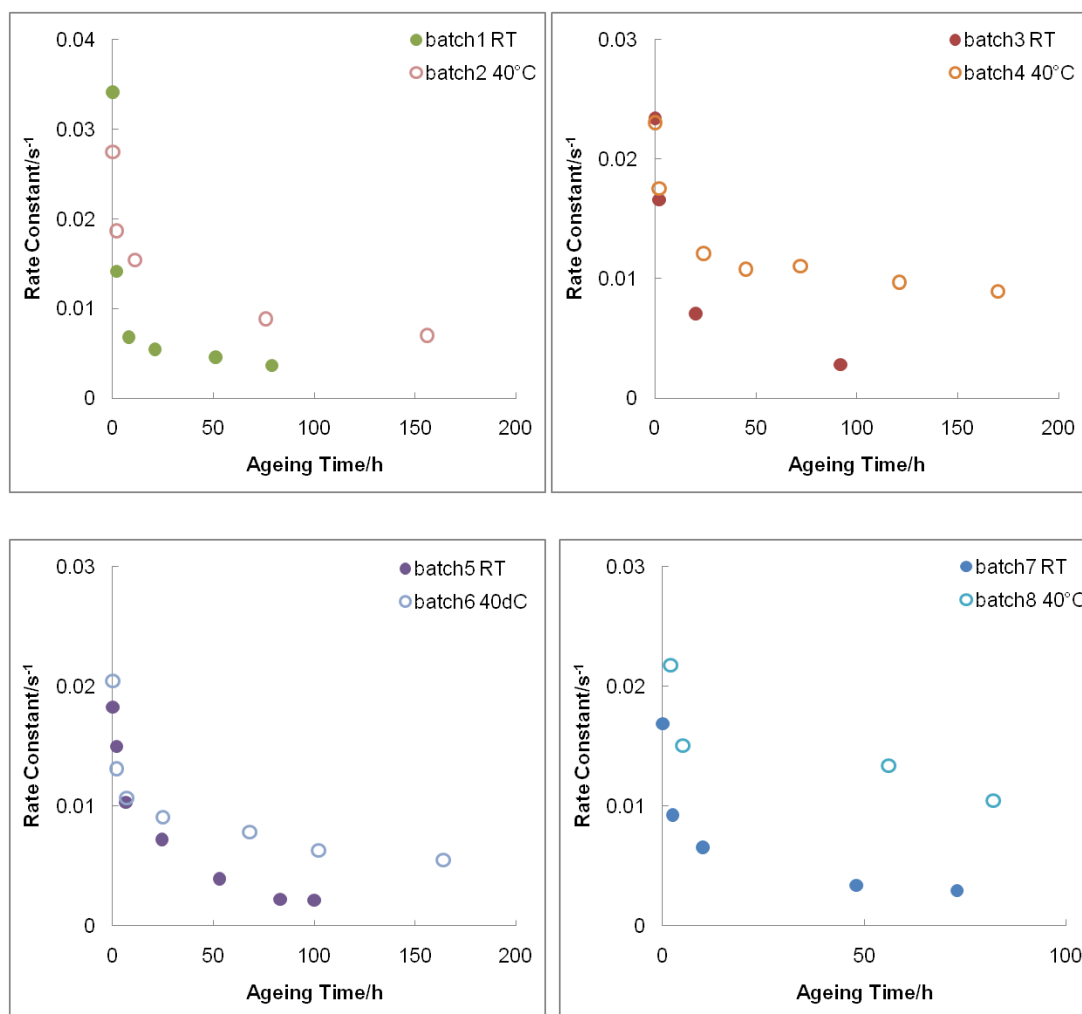


**Figure 2. 11. Effect of ageing on the rate of ligand exchange at different reaction temperature.**

By analyzing the kinetic data of fresh and aged AuNPs from different batches, it was found that in general, the reduction of reactivity was more significant if ligand exchange was carried out at lower temperature (Table 2.1).

**Table 2. 1. Effect of ageing on C<sub>4</sub>S-AuNPs.**

AuNPs	Reaction temperature	Hours aged	$k_{\text{fresh}}/k_{\text{aged}}$
batch1	RT	79	9.35
batch3	RT	92	8.33
batch5	RT	100	8.50
batch7	RT	73	5.74
batch2	40 °C	156	3.91
batch4	40 °C	170	2.58
batch6	40 °C	164	3.72
batch8	40 °C	82	2.08

We thus conclude that ligand exchange becomes more temperature-dependent as the time of ageing increases. Assuming that ageing is due to annealing of reactive sites on AuNPs, as AuNPs are aged, this process leads to formation of more coordinated sites, therefore ligand dissociation from such sites results in higher entropy change. Hence, aged AuNPs are more sensitive to reaction temperature.

#### 2.4.2.3. Outgoing ligand dependence of ageing effect

The effect of protecting ligand on ligand exchange reaction was reported<sup>72</sup> by Murray and co-workers. AuNPs protected by short chain thiolates were found to be more ‘exchangeable’, in terms of faster reaction rate with thiols and larger extent of exchange. The effect was interpreted as higher thermodynamic stability of long chain thiolates attached on gold surface. Due to the important role of ligand chain length in exchange reactions, the ligand dependence of ageing effect was studied.

As stated in Section 2.4.1.3 (p50), the ligand exchange reaction of *n*-octanethiol protected AuNPs (C<sub>8</sub>S-AuNPs) and DIS3 was undertaken at room temperature (*e.g.* 20 °C) using a 1:1 AuNP/ligand ratio. The reactions were found to be slower than C<sub>4</sub>S-AuNPs, and a clear decay of reaction rate was also observed with increasing ageing time (Figure 2.12). Fresh C<sub>8</sub>S-AuNPs were found to react more than 6 times as fast as particles aged for 185 hours.

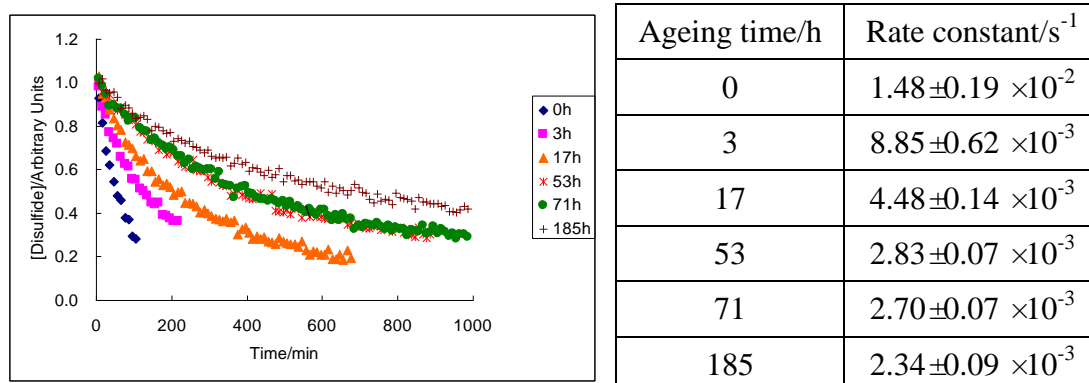


**Figure 2. 12.** Normalized kinetic profiles and rate constants of ligand exchange reactions of C<sub>8</sub>S-AuNPs and DIS3 with 1:1 ratio, at room temperature.

The C<sub>8</sub>SH ligand roughly has the same length as the thiolate branch in DIS3. We further increased the chain length of the protecting ligand, employing *n*-octadecanethiol protected AuNPs (C<sub>18</sub>S-AuNPs) in the ageing study. Their reaction with DIS3 at a 1:1 AuNP/ligand ratio was also monitored at room temperature. As expected, a similar ageing effect was observed. The reaction rate of fresh C<sub>18</sub>S-AuNPs was 3 times faster than particles aged for 174h (Figure 2.13).

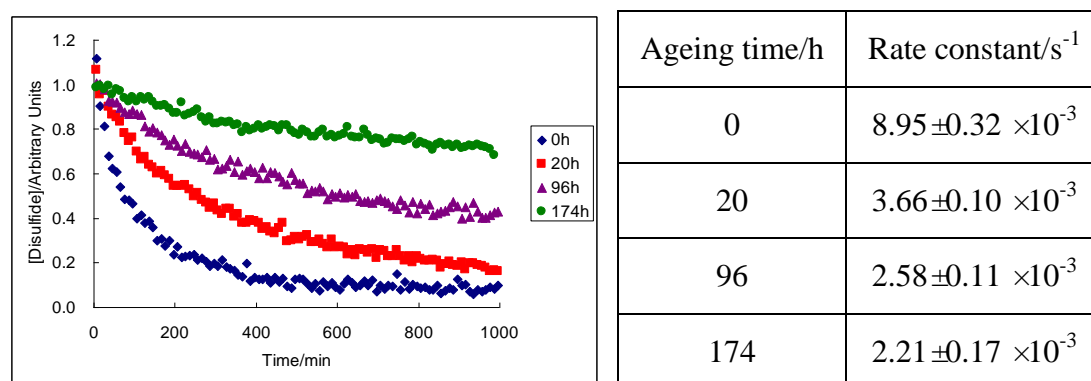


**Figure 2. 13.** Normalized kinetic profiles and rate constants of ligand exchange reactions of C<sub>8</sub>S-AuNPs and DIS3 with 1:1 ratio, at room temperature.

By comparing the reaction rates of C<sub>4</sub>S-, C<sub>8</sub>S- and C<sub>18</sub>S-AuNPs (Figure 2.14), a few interesting observations were made. Firstly, the reactivity of fresh AuNPs showed strong dependence on the chain length of the protecting thiolate ligand, but for aged particles the reaction rates of AuNPs with different protecting ligand are similar. The effect of AuNPs chain length on the reaction rate of ligand exchange with DIS3 exists for fresh particles only. Secondly, ageing mostly depends on the first day or

even a few hours after the AuNPs were prepared. Sharp decreases of reaction rate can be observed in the first few hours of ageing, then the rates level off. This effect is independent to the chain length of the protecting ligand.

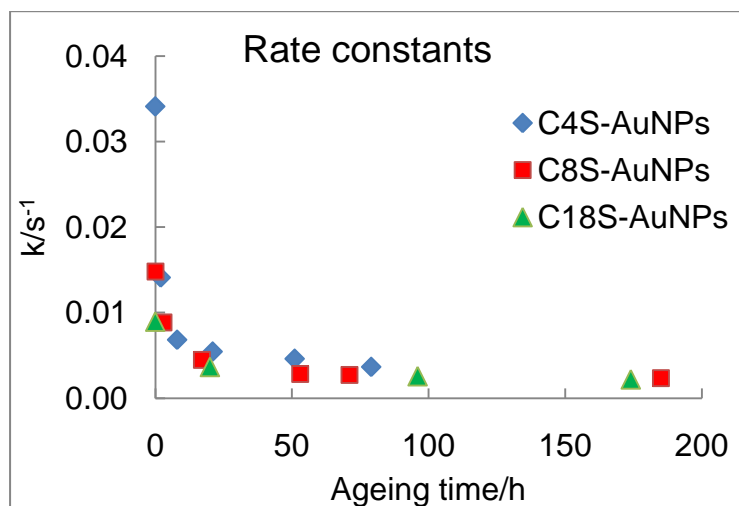


**Figure 2. 14. Reduced reaction rate of aged C<sub>4</sub>S-, C<sub>8</sub>S and C<sub>18</sub>S-AuNPs in ligand exchange reactions with DIS3.**

For fresh particles, chain length of the leaving thiolate ligand has significant effect on the reaction rate. Since dissociation is the rate-determine step, this observation suggests that desorption of thiolate ligand from fresh AuNPs depends on the chain length. For aged particles, the effect of the chain length on reactivity was found to be minimal. These observations are consistent with the presence of different sites on Au surface. Considering defect sites on AuNPs surface as less coordinated gold atoms, ligand desorption from these sites requires less free energy than the staple-like gold thiolates. SAM formation of long chain thiols is slower and therefore results in fewer kinetically-trapped defects. The defect sites on the surface of nanoparticles protected by long chain thiolates are less reactive. Ageing is possibly due to surface reorganization. As AuNPs are aged, the defect gold thiolates are better coordinated hence require more free energy to desorb. Hence, the chain length dependence of the reaction rate is smaller.

### 2.4.3. Ageing and concurrent size variation of AuNPs

Ageing of AuNPs results in reduced reactivity in ligand exchange reaction with disulfides. In order to understand the origin of the ageing effect, it is important to know the concurrent changes to the AuNPs, particularly particle size. Therefore, the size of AuNPs was monitored by Transmission Electron Microscopy (TEM). No size change was observed for C<sub>4</sub>S-AuNPs aged in a chlorobenzene solution for 4 weeks. Taking into account that TEM images cannot reveal small changes of particle size, UV-*vis* spectroscopy was used to monitor the particle size changes during ageing, due to its sensitivity to the surface plasmon band of AuNPs. A typical UV spectrum of AuNPs in solution is shown in Figure 2.4 (p46). A shoulder around 520nm is the characteristic surface plasmon peak of AuNPs in solution. Position and intensity of the peak depend on particle size.

C<sub>4</sub>S-AuNPs were synthesized and aged in a 10<sup>-4</sup> M chlorobenzene solution. At different ageing times, aliquots of the AuNPs solution were taken and diluted to 5×10<sup>-7</sup> M, thus UV spectra of AuNPs of different ageing time were obtained (Figure 2.15). Only random variations to the surface plasmon band of AuNPs were found, probably due to slight difference in concentration. The result suggests that size of AuNPs does not change with ageing within experimental error.

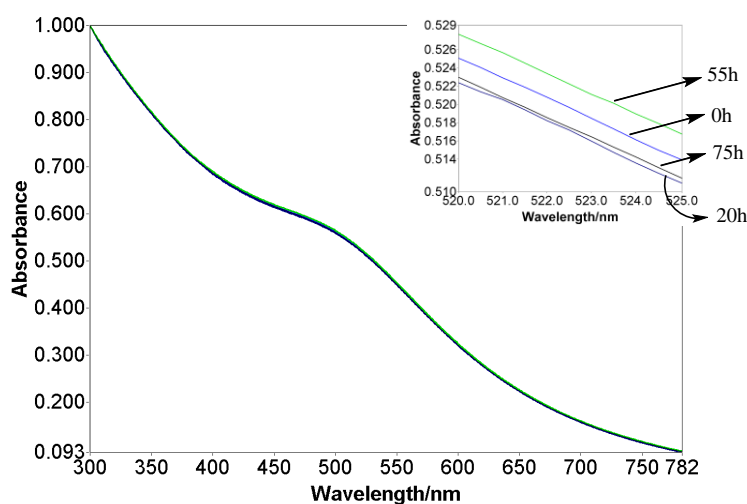
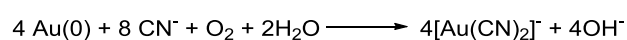


Figure 2. 15. UV-vis spectra of C<sub>4</sub>S-AuNPs of different ageing times.

#### 2.4.4. Reduced reactivity of aged AuNPs in cyanide induced decomposition

Since no concurrent size variations were observed during ageing, it is likely that the effect of ageing is related to the presence of different binding sites and surface coverage on AuNPs. Apart from ligand exchange reaction, the rate of cyanide induced AuNP decomposition also depends on the presence of defect sites and surface protection. Cyanide can etch gold in the presence of O<sub>2</sub>. In this process, Au(0) is oxidized to Au(I) by oxygen and cyanide acts as a ligand for the released Au(I) ions (Scheme 2.11).



**Scheme 2. 11. Etching of gold by molecular oxygen in the presence of cyanide.**

Studies<sup>97-99</sup> of alkanethiolate SAMs on flat Au surface suggest that cyanide facilitates the dissociation of thiolate ligands and etches the gold layer. Murray *et al.* also observed<sup>74</sup> that the rate of cyanide induced etching of thiolate AuNPs decreased with increasing thiolate chain length. Here, we adopted this reaction to investigate the defect sites on AuNPs and defect-related ageing effect.

C<sub>4</sub>S-AuNPs were synthesized as previously stated and aged in a 10<sup>-4</sup> M chlorobenzene solution. At different ageing times, aliquots of the AuNPs solution were taken, dried under a flow of N<sub>2</sub> gas, and re-dissolved in THF to make a 2×10<sup>-6</sup> M solution. Then the solution was mixed with aqueous KCN (3.5×10<sup>-4</sup> M) in a 1:1 (v/v) ratio. The resulting mixture contained AuNPs and a 10-fold excess of CN<sup>-</sup>. Since the surface plasmon band at 520nm does not change with ageing, cyanide induced decomposition of AuNPs was monitored by UV-*vis* spectroscopy. Following addition of cyanide to the THF solution of AuNPs, time-scans at 520 nm were performed to generate kinetic profiles (Figure 2.16).

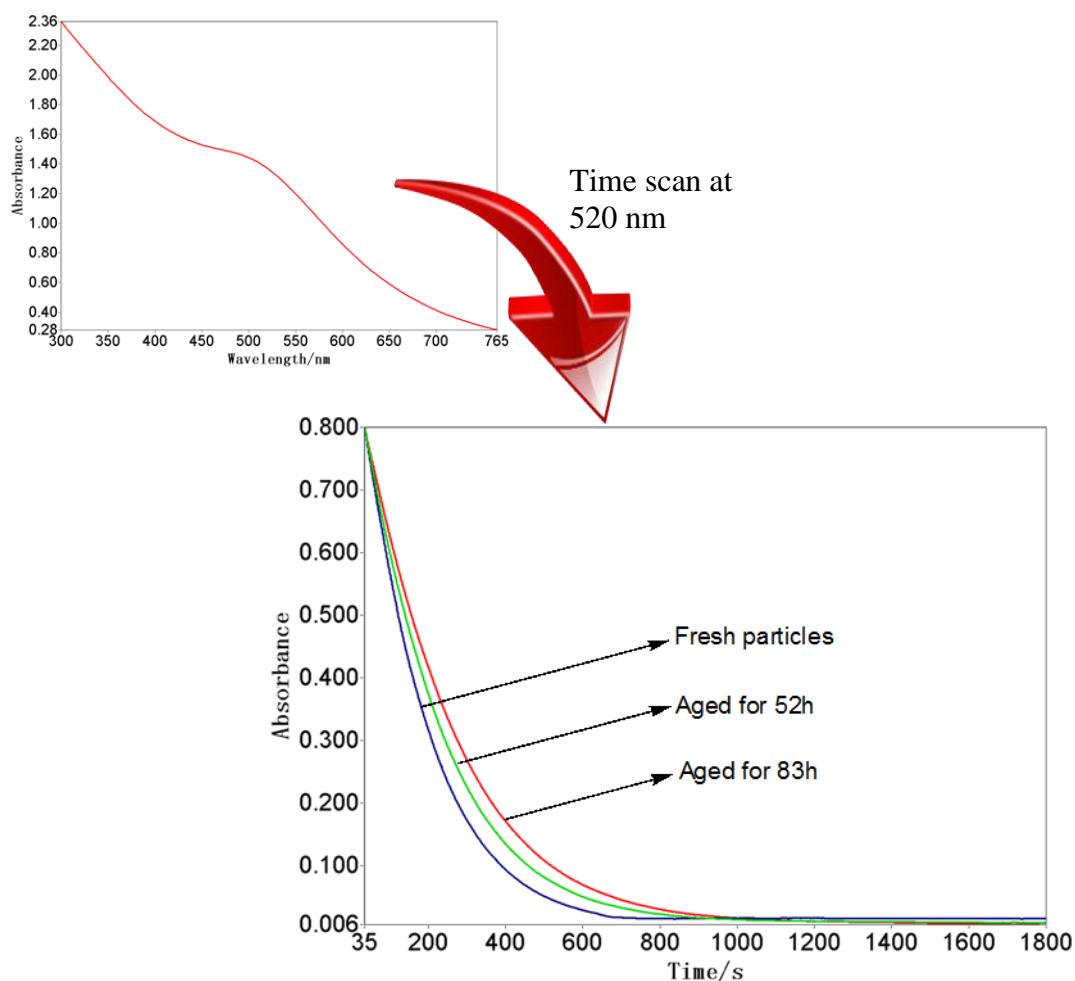


**Figure 2. 16. Kinetic profiles of  $C_4S$ -AuNP decomposition in the presence of  $CN^-$ , monitored by UV-*vis* spectroscopy via time scans at 520nm.**

As shown in Figure 2.16, reduced reactivity of aged AuNPs in cyanide induced decomposition was also observed. It is plausible that cyanide induced decomposition also starts from defect sites on AuNPs. In aged particles, due to surface reorganization, the density of such defect sites is much lower. Therefore, the reaction rate of aged AuNPs in cyanide induced decomposition is slower. We also noticed that in this reaction, the effect of ageing is not as significant as observed in ligand exchange with disulfides. Ageing for 83 hours resulted in only 30% lower reaction rate (Table 2.2).

**Table 2. 2. 1<sup>st</sup> order rate constants of cyanide induced decomposition of C<sub>4</sub>S-AuNPs.**

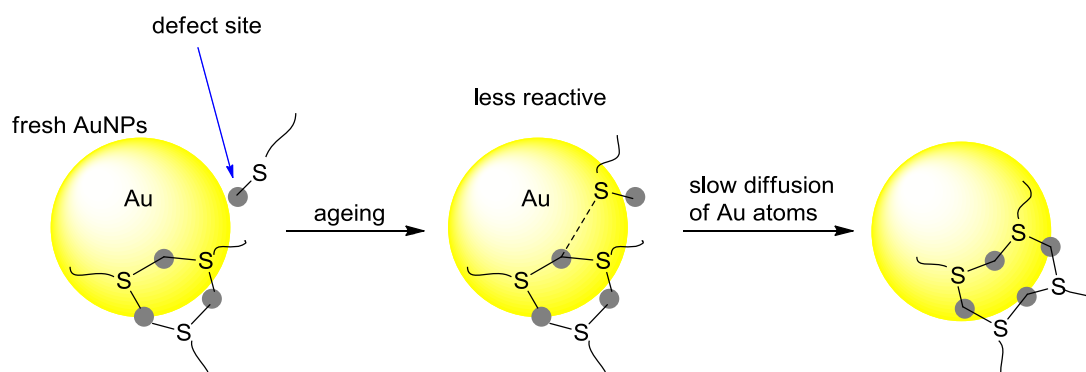
Time of ageing/h	1 <sup>st</sup> order rate constant/s <sup>-1</sup>	k <sub>aged</sub> /k <sub>fresh</sub>
0	5.70×10 <sup>-3</sup>	/
52	4.69×10 <sup>-3</sup>	0.82
83	4.16×10 <sup>-3</sup>	0.73

Ageing of AuNPs seems to have different effect on the rate of different reactions. In ligand exchange reactions with disulfide, ageing of C<sub>4</sub>S-AuNPs resulted in a 10-fold decrease in the reaction rate. Aged C<sub>4</sub>S-AuNPs only resulted in a 30% lower reaction rate in the cyanide induced decomposition. The results from our group suggest that ageing does not affect the ligand exchange with thiols. The reason for these different observations is probably due to different mechanism of these reactions. For reactions taking place primarily at the defect sites of AuNPs (*e.g.* ligand exchange with disulfides), ageing significantly reduces the reaction rate. In the cyanide induced decomposition of AuNPs, the reaction probably starts from defect sites. However, the reaction is not limited to the defect sites. Therefore, slower reaction rate was observed but the effect is less significant. In the ligand exchange reaction of AuNPs with thiols, the mechanism probably does not depend on the presence of defect sites.

#### 2.4.5. Conclusions on ageing effect of AuNPs

In summary, ageing is a general feature of AuNPs. We have demonstrated that this effect does not depend on reaction temperature and the protecting ligand. Reduced reactivity was observed for aged AuNPs in defect-related reactions including cyanide induced AuNP decomposition and ligand place-exchange reactions. Ligand exchange reaction of thiolate protected AuNPs with disulfide was confirmed to be a 1<sup>st</sup> order, dissociative process. The reactivities of fresh and aged AuNPs with different thiolate ligands and at different reaction temperature are consistent with the presence of different binding sites on AuNPs. These sites are probably located in the ‘outer’ shell of AuNPs. As the crystal structures<sup>63-64</sup> of monolayer thiolate protected AuNPs suggest, the Au core is protected by several ‘different’ gold atoms in the outer shell which are networked via the thiolate ligands. We propose that freshly made AuNPs have several defect sites on the Au surface. The number of such sites

strongly depends on the synthetic procedure and thus varies from batch to batch. These defect sites are likely to be located in the outer shell of AuNPs, but are less coordinated and networked with other gold atoms and thiolate ligands (*e.g.* gold thiolates are only bonded to the Au core). The isolated gold thiolates are labile, and hence are kinetically reactive. The free energy required to desorb the defect gold thiolates is smaller than for the staple-like gold thiolates, hence the disulfide exchange which requires higher activation energy than for thiol exchange is only observed on the defect sites. Ageing can be considered as a surface reorganization process: the defect sites become better coordinated with other gold atoms, which reduces the reactivity of these sites. The lateral diffusion of gold thiolates is slow<sup>87</sup>, therefore surface rearrangement cannot take place quickly. But in the long run, the defects slowly diffuse to adjoin the other Au atoms and engage in the network (Scheme 2.12).



**Scheme 2. 12. Schematic of ageing effect of thiolate protected AuNPs. Gold core is shown in yellow, surrounding gold atoms are represented by grey dots.**

Desorption of the defect gold thiolates is likely to cause minimal entropy change since it does not affect the staple-like gold thiolate network. Hence, ligand desorption from defect sites is not greatly affected by reaction temperature. Ligand desorption from the better coordinated gold thiolate involves breaking the gold thiolates network, and thus may result in a higher entropy change. Therefore, as AuNPs are aged, the temperature dependence of the rate of ligand exchange becomes more significant. The rate of SAM formation also depends on the chain length of the protecting ligand, and thus leads to different reactivity of the kinetically-trapped defect sites. As AuNPs are aged, the defect sites become weakly bonded to the other gold atoms. Free energy required to break the gold thiolates network during ligand

desorption dominates the energy hurdle, therefore the reactivity of aged C<sub>4</sub>S-, C<sub>8</sub>S- and C<sub>18</sub>S-AuNPs is similar.

These arguments could explain the ageing effect and ligand desorption from fresh and aged particles, but a comprehensive understanding is still lacking. Although X-ray structures of the thiolate monolayer unambiguously show the networked gold atoms in the outer shell of Au core, the proposed defect sites (*e.g.* less coordinated) cannot be revealed by the crystal structures. There are also many unanswered questions which are fundamental to the understanding of AuNP behaviour and their reactions. For instance, the ligand exchange of AuNPs with thiols and disulfides appears to proceed by different mechanisms but details are vague. We do not expect to answer these questions but in order to achieve a better understanding, next section considers extent of ligand exchange.

## **2.5. Extent of ligand exchange reactions of AuNPs with disulfides**

We hypothesized that the ageing of AuNPs and associated reduced reactivity is due to the reorganization of defect sites on the particles. However, many fundamental aspects of the ageing effect, and mechanism of ligand exchange is not known. The maximum extent of ligand exchange is related to the different binding sites and detailed mechanism of the reaction. It is also important to know the effect of ageing on the number of reactive binding sites on AuNPs. Therefore, the extent of ligand exchange reactions was studied.

### **2.5.1. Does maximum extent of ligand exchange reaction change with ageing?**

In order to understand the effect of ageing on the maximum extent of ligand exchange, the reaction of C<sub>4</sub>S-AuNPs and DIS3 with AuNP/DIS3 in a 1:10 ratio (as described in Section 2.4.2.2, p53) was studied. The reaction was monitored at 40 °C

to accelerate the reaction. A high ratio of DIS3 was used in order to ensure that disulfide is in excess at the end of the reaction, and thus the extent of reaction can be determined. Figure 2.17 shows a typical kinetic curve of this reaction. The excess DIS3 can be detected at the end of the reaction.

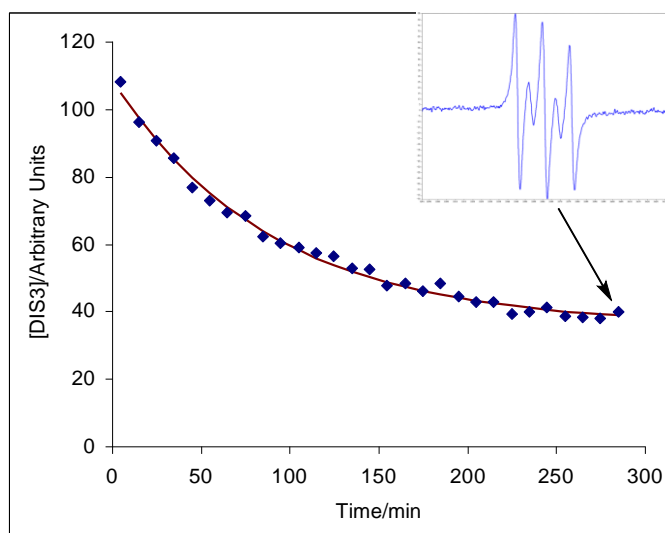


**Figure 2. 17. Kinetic profile of ligand exchange reaction C<sub>4</sub>S-AuNPs and DIS3 at 40 °C, using a molar ratio of 1:10. EPR spectrum at the end of the reaction clearly suggest presence of DIS3, therefore proved the reaction did not go to completion.**

The kinetic profiles of the reaction undertaken at different ageing times were fitted to 1<sup>st</sup> order kinetic model and extrapolated to obtain the estimated maximum extent of ligand exchange. The percentage of DIS3 reacted was calculated from the simulation (Table 2.3).

**Table 2. 3. Maximum extent of ligand exchange of C<sub>4</sub>S-AuNPs and DIS3 with a ratio of 1:10 at 40 °C.**

Ageing time	Percentage DIS3 reacted	Number of ligand exchanged per particle
0h	60.30%	6.03
7h	60.54%	6.05
25h	57.64%	5.76
68h	52.75%	5.27
102h	55.25%	5.53
164h	60.14%	6.01

As shown in Table 2.3, it is clear that the proportion of reacted DIS3 did not change within experimental error. In average, 6 ligands were exchanged per particle. This observation was found to be reproducible. However, the number of ligand exchanged per particle seems to be batch dependent. This result is consistent with the batch-dependent number of defect sites on AuNPs.

### 2.5.2. AuNP/disulfide ratio dependence on the maximum extent of ligand exchange reactions

In order to understand how the ratio of AuNP/incoming ligand affects the maximum extent of exchange (*e.g.* does the extent of exchange increase with higher concentration of disulfide), the reaction was carried out with different AuNP/DIS3 ratios. Ligand exchange of 2-week-old C<sub>4</sub>S-AuNPs and DIS3 in 1:3, 1:5, 1:10, 1:20 and 1:30 ratios was carried out at 50 °C. The reaction was monitored by EPR spectroscopy and kinetic profiles were thus obtained (Figure 2.18).

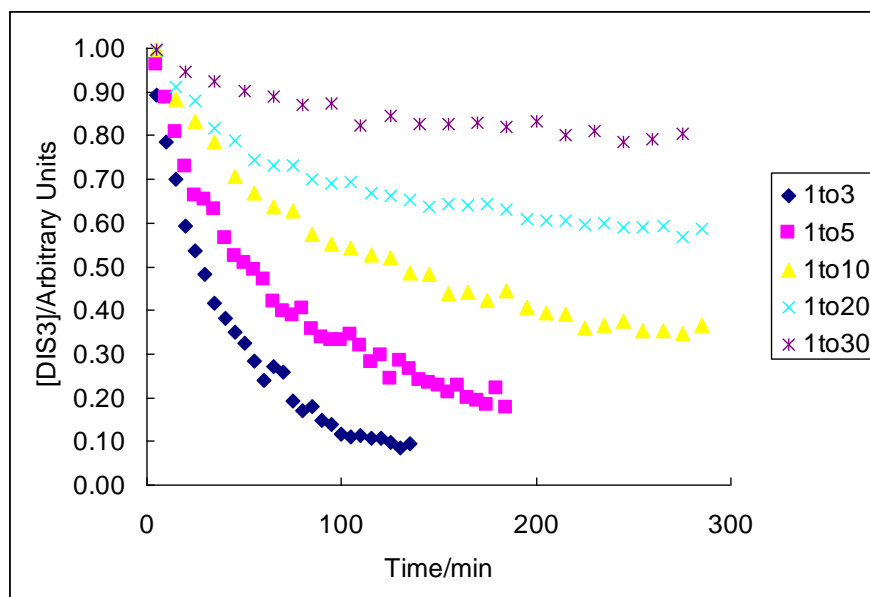


**Figure 2. 18.** Normalized kinetic profiles of the ligand exchange reaction of C<sub>4</sub>S-AuNPs and DIS3 with various molar ratios at 50 °C.

Using the same procedure, the maximum number of exchangeable ligands per particle was calculated from fitting to a 1<sup>st</sup> order kinetic model (Table 2.4). In

reactions with 1:3 and 1:5 AuNP/DIS3 ratio, almost all DIS3 was consumed. In the exchange with higher DIS3 ratio (1:10, 1:20 and 1:30), additional amount of DIS3 did not promote the exchange reaction, therefore the maximum extent of reaction does not depend on the AuNP/disulfide ratios. The number of exchanged ligands is batch dependent. In this batch, C<sub>4</sub>S-AuNPs have *ca.* 7 exchangeable binding sites per particle.

**Table 2. 4. Number of exchanged thiolate ligands per particle in ligand exchange reactions starting with different AuNP/DIS3 ratio.**

AuNP/DIS3 ratio	Number of thiolate exchanged per particle
1:3	2.77
1:5	4.55
1:10	6.71
1:20	7.41
1:30	6.41

Therefore, it is possible to conclude that the number of reactive sites on AuNPs does not depend on ageing or excess incoming ligand.

### 2.5.3. The extent of ligand exchange reaction at different temperature

The investigation of ligand exchange reactions of AuNPs with disulfides suggests the presence of reactive defect sites. It is likely that there are different types of binding sites on the Au surface with different reactivity. At low temperature, only the most reactive sites (*e.g.* defects) participate in the exchange reaction. However, other sites might also become reactive at higher temperature. The maximum extent of the ligand exchange reaction was found to be independent of ageing presumably because the number of defect sites does not change with ageing. However, at higher temperature, more sites could be activated. In order to understand the reactivity of different binding sites on AuNPs, ligand exchange of C<sub>4</sub>S-AuNPs with DIS3 at different temperature (*e.g.* 30 °C, 50 °C, 70 °C and 90 °C) was monitored by EPR spectroscopy (Figure 2.19). The reaction was carried out as previously described, using a 1:20 AuNP/DIS3 ratio, to allow engagement of additional binding sites in the ligand exchange.

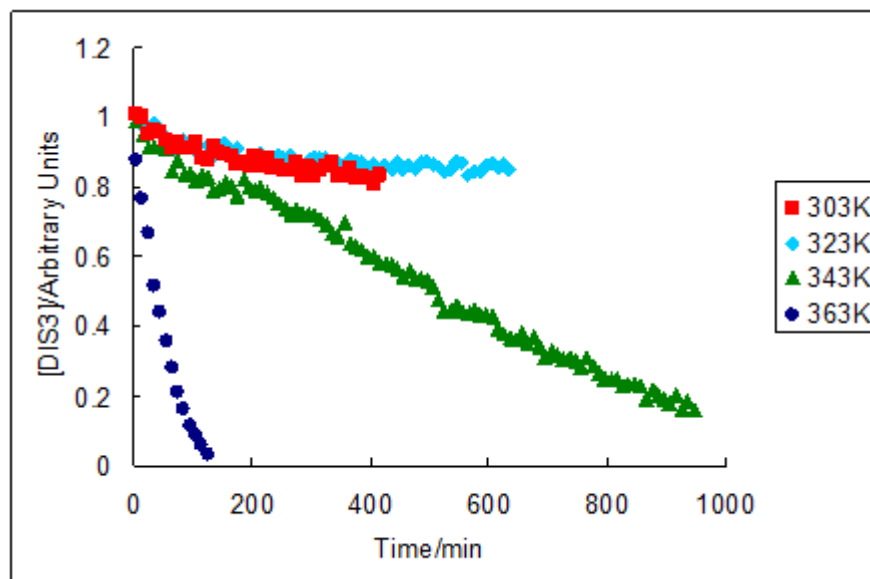


**Figure 2. 19.** Kinetic profiles of the ligand exchange reaction of C<sub>4</sub>S-AuNPs and DIS3 in a 1:20 ratio at 30, 50, 70 and 90 °C.

As shown in Figure 2.19, maximum extent of ligand exchange reaction increased with increasing temperature. The reactions undertaken at 70 and 90 °C engaged more binding sites and reaction went to completion whilst the reactions at 30 and 50 °C did not. In addition, the reactions at high temperature did not follow 1<sup>st</sup> order but appeared to be zeroth order. This result confirms presence of different binding sites on AuNPs. Hence, the overall reaction should be described by two (or more) processes. At room temperature, the slower reactions are negligible. As a result, the kinetic profiles fit standard 1<sup>st</sup> order kinetics model. At higher temperature, the rate of the slower process increases significantly and can even dominate the overall kinetics. Therefore the kinetic profiles do not follow 1<sup>st</sup> order kinetics and the maximum extent of ligand exchange increases.

#### **2.5.4. Conclusions on extent of ligand exchange**

The maximum extent of ligand exchange was found to be independent of ageing of AuNPs and the concentration of incoming ligand. However, ligand exchange reaction carried out at higher temperature (*e.g.* 70 °C) significantly increased the extent of exchange, and also changed the kinetic behaviour of the reaction. These

observations can be explained by the presence of different binding sites on AuNPs. Only the most reactive sites (*e.g.* defect sites) are engaged in the ligand exchange reactions with disulfides at lower temperature (*e.g.* room temperature). Other sites (*e.g.* gold thiolate ‘staples’) probably require higher activation enthalpy and thus are less reactive. The reaction of these sites with disulfides is very slow (if any) at room temperature, therefore such sites can be considered as unreactive.

A major difference between ligand exchange with disulfides and thiols is the maximum extent of exchange. Murray *et al.* reported<sup>71</sup> that 2/3 of the ligands on C<sub>4</sub>S-AuNPs can be replaced in the reaction with thiols. We detected *ca.* 5% ligand exchange of C<sub>4</sub>S-AuNPs with disulfide at 50 °C. Such a substantial difference can be explained by the different reaction mechanisms of ligand exchange with thiols and disulfides. In the reaction with disulfides, gold thiolate ‘staples’ are not reactive at room temperature. These sites can only react at forcing conditions (*e.g.* elevated temperature). In fact, disulfides were initially reported as unreactive with AuNPs<sup>71</sup>, probably due to the small extent of exchange and slow reaction rate, particularly if AuNPs were sufficiently aged. In contrast, the gold thiolate ‘staples’ are probably reactive in the ligand exchange with thiols. The ligand exchange of AuNPs with thiols is a bimolecular process, in which adsorption of the incoming ligand to the gold atoms facilitates desorption of the outgoing ligand. Hence, the extent of ligand exchange is much larger in reactions with thiols. The stable sites far outnumber the defect sites on AuNPs. Since ligand exchange reaction of AuNPs with thiols utilizes the less reactive gold thiolate ‘staples’, annealing of the defect sites is dwarfed by the predominant reaction and is not detectable. Unpublished result from our lab shows that ageing effect is not observed in ligand exchange reactions of AuNPs with thiols, which is consistent with the different mechanisms of ligand exchange with thiols and disulfides.

## 2.6. Conclusions

This chapter details the investigations of ageing of thiolate coated AuNPs and mechanism of ligand exchange reactions. We have observed reduced reactivity of aged AuNPs in defect-related reactions, including ligand exchange with disulfides and cyanide induced AuNP decomposition. The effect of ageing was found to be a general feature of AuNPs, which was attributed to surface reorganization and diminishing number of defect sites. We propose that fresh AuNPs have defect sites (*e.g.* flexible gold thiolates) in the outer layer which are not networked with the gold ‘staples’. The bond of ‘defect’ gold thiolates with the Au core has lower enthalpy and as a result, these sites are more labile. Desorption of the isolated ‘defect’ gold thiolates also results in lower entropy change as compared to the networked gold staples. The thermodynamics of the different binding sites on AuNPs determine the reactivity and Arrhenius behaviour. The reaction of AuNPs with disulfides depends on dissociation of gold thiolates, and hence depends on the number of labile gold thiolates on Au core. Ageing is a surface reorganization process in which the ‘defect’ gold thiolates are better coordinated and connected with the other gold atoms. Diffusion of Au atoms is slow therefore the labile gold thiolates do not network with the gold staples, leading to retardation but not inhibition of these sites. Nonetheless, in the long run, the gold atoms can be reorganized to be engaged in the networked ‘staples’ in perfectly aged AuNPs (*e.g.* AuNPs crystal). The networked gold thiolate staples bond with AuNPs more strongly and require higher free energy to dissociate, therefore they only react with disulfide at forcing conditions (*e.g.* elevated temperature).

**References:**

1. G. A. Mansoori, *Principles of Nanotechnology: Molecular-Based Study Of Condensed Matter In Small Systems*, World Scientific Publishing Co., Singapore, 2005.
2. G. Schmid, ed., *Nanoparticles: From Theory To Application*, WILEY-VCH Verlag GmbH & Co. KGaA, Weinheim, 2004.
3. C. N. R. Rao, A. Muller and A. K. Cheetham, eds., *Nanomaterials Chemistry: Recent Developments and New Directions*, WILEY-VCH Verlag GmbH & Co. KGaA, Weinheim, 2007.
4. C. Burda, X. Chen, R. Narayanan and M. a. El-Sayed, *Chem. Rev.*, 2005, **105**, 1025-1102.
5. R. P. Feynman, in *The Pleasure of Finding Things Out: The Best Short Works of Richard P. Feynman*, ed. J. Robbins, Perseus Books, New York, Editon edn., 1999.
6. S. Eustis and M. A. El-Sayed, *Chem. Soc. Rev.*, 2006, **35**, 209-217.
7. J. C. Slater, *J. Chem. Phys.*, 1964, **41**, 3199-3204.
8. M. C. Daniel and D. Astruc, *Chem. Rev.*, 2004, **104**, 293-346.
9. M. Faraday, *Phil. Trans. R. Soc. London*, 1857, **147**, 145-181.
10. D. H. Brown and W. E. Smith, *Chem. Soc. Rev.*, 1980, **9**, 217-240.
11. G. Frens, *N. Ph. S.*, 1973, **241**, 20-22.
12. G. Schmid, *Chem. Rev.*, 1992, **92**, 1709-1727.
13. J. Turkevich, P. C. Stevenson and J. Hillier, *Discuss. Faraday Soc.*, 1951, 55-75.
14. M. Valden, X. Lai and D. W. Goodman, *Science*, 1998, **281**, 1647-1650.
15. M. Haruta, T. Kobayashi, H. Sano and N. Yamada, *Chem. Lett.*, 1987, 405-408.
16. M. Haruta, N. Yamada, T. Kobayashi and S. Iijima, *J. Catal.*, 1989, **115**, 301-309.
17. M. Haruta, S. Tsubota, T. Kobayashi, H. Kageyama, M. J. Genet and B. Delmon, *J. Catal.*, 1993, **144**, 175-192.
18. H. Sakurai, S. Tsubota and M. Haruta, *Appl. Catal., A.*, 1993, **102**, 125-136.
19. M. Haruta, *Catal. Today*, 1997, **36**, 153-166.
20. D. J. Gorin and F. D. Toste, *Nature*, 2007, **446**, 395-403.

21. A. S. K. Hashmi and G. J. Hutchings, *Angew. Chem. Int. Ed.*, 2006, **45**, 7896-7936.
22. M. Haruta, *Cattech*, 2002, **6**, 102-115.
23. G. C. Bond and D. T. Thompson, *Cat. Rev. - Sci. Eng.*, 1999, **41**, 319-388.
24. R. Narayanan and M. A. El-Sayed, *J. Phys. Chem. B*, 2005, **109**, 12663-12676.
25. C. Buzea, Pacheco, II and K. Robbie, *Biointerphases*, 2007, **2**, MR17-MR71.
26. G. Oberdorster, *J. Intern. Med.*, 2010, **267**, 89-105.
27. E. E. Connor, J. Mwamuka, A. Gole, C. J. Murphy and M. D. Wyatt, *Small*, 2005, **1**, 325-327.
28. N. Lewinski, V. Colvin and R. Drezek, *Small*, 2008, **4**, 26-49.
29. Y. Pan, S. Neuss, A. Leifert, M. Fischler, F. Wen, U. Simon, G. Schmid, W. Brandau and W. Jahnke-Dechent, *Small*, 2007, **3**, 1941-1949.
30. C. Sönnichsen, T. Franzl, T. Wilk, G. v. Plessen and J. Feldmann, *N. J. Ph.*, 2002, **4**, 93.91-93.98.
31. G. R. Souza, D. R. Christianson, F. I. Staquicini, M. G. Ozawa, E. Y. Snyder, R. L. Sidman, J. H. Miller, W. Arap and R. Pasqualini, *Proc. Natl. Acad. Sci. U.S.A.*, 2006, **103**, 1215-1220.
32. D. Boyer, P. Tamarat, A. Maali, B. Lounis and M. Orrit, *Science*, 2002, **297**, 1160-1163.
33. X. Huang, P. Jain, I. El-Sayed and M. El-Sayed, *Laser Med. Sci.*, 2008, **23**, 217-228.
34. C. Alric, J. Taleb, G. Le Duc, C. Mandon, C. Billotey, A. Le Meur-Herland, T. Brochard, F. Vocanson, M. Janier, P. Perriat, S. Roux and O. Tillement, *J. Am. Chem. Soc.*, 2008, **130**, 5908-5915.
35. J. F. Hainfeld, D. N. Slatkin, T. M. Focella and H. M. Smilowitz, *Br. J. Radiol.*, 2006, **79**, 248-253.
36. M. F. Warsi, R. W. Adams, S. B. Duckett and V. Chechik, *Chem. Commun.*, 2010, **46**, 451-453.
37. I. El-Sayed, X. Huang, F. Macheret, J. O. Humstoe, R. Kramer and M. El-Sayed, *Technol. Cancer Res. Treat.*, 2007, **6**, 403-412.
38. P. Ghosh, G. Han, M. De, C. K. Kim and V. M. Rotello, *Advanced Drug Delivery Reviews*, 2008, **60**, 1307-1315.

39. G. F. Paciotti, D. G. I. Kingston and L. Tamarkin, *Drug Dev. Res.*, 2006, **67**, 47-54.
40. G. F. Paciotti, L. Myer, D. Weinreich, D. Goia, N. Pavel, R. E. McLaughlin and L. Tamarkin, *Drug Deliv.*, 2004, **11**, 169-183.
41. D. Astruc, M. C. Daniel and J. Ruiz, *Chem. Commun.*, 2004, 2637-2649.
42. M. T. Castaneda, S. Alegret and A. Merkoci, *Electroanalysis*, 2007, **19**, 743-753.
43. U. H. F. Bunz and V. M. Rotello, *Angew. Chem. Int. Ed.*, 2010, **49**, 3268-3279.
44. G. Raschke, S. Kowarik, T. Franzl, C. Sonnichsen, T. A. Klar, J. Feldmann, A. Nichtl and K. Kurzinger, *Nano Lett.*, 2003, **3**, 935-938.
45. L. Pasquato, P. Pengo and P. Scrimin, *J. Mater. Chem.*, 2004, **14**, 3481-3487.
46. A. Labande, J. Ruiz and D. Astruc, *J. Am. Chem. Soc.*, 2002, **124**, 1782-1789.
47. X. H. Ji, X. N. Song, J. Li, Y. B. Bai, W. S. Yang and X. G. Peng, *J. Am. Chem. Soc.*, 2007, **129**, 13939-13948.
48. J. Polte, T. T. Ahner, F. Delissen, S. Sokolov, F. Emmerling, A. F. Thunemann and R. Kraehnert, *J. Am. Chem. Soc.*, 2010, **132**, 1296-1301.
49. B.-K. Pong, H. I. Elim, J.-X. Chong, W. Ji, B. L. Trout and J.-Y. Lee, *J. Phys. Chem. C*, 2007, **111**, 6281-6287.
50. G. Schmid and B. Corain, *Eur. J. Inorg. Chem.*, 2003, 3081-3098.
51. M. Brust, J. Fink, D. Bethell, D. J. Schiffrin and C. Kiely, *J. Chem. Soc., Chem. Commun.*, 1995, 1655-1656.
52. M. Brust, D. Bethell, D. J. Schiffrin and C. J. Kiely, *Adv. Mater.*, 1995, **7**, 795-797.
53. M. Brust, M. Walker, D. Bethell, D. J. Schiffrin and R. Whyman, *J. Chem. Soc., Chem. Commun.*, 1994, 801-802.
54. G. Schmid, R. Pfeil, R. Boese, F. Bandermann, S. Meyer, G. H. M. Calis and W. A. Vandervelden, *Chem. Ber. Recl.*, 1981, **114**, 3634-3642.
55. W. W. Weare, S. M. Reed, M. G. Warner and J. E. Hutchison, *J. Am. Chem. Soc.*, 2000, **122**, 12890-12891.
56. K. R. Brown, L. A. Lyon, A. P. Fox, B. D. Reiss and M. J. Natan, *Chem. Mater.*, 2000, **12**, 314-323.
57. K. R. Brown and M. J. Natan, *Langmuir*, 1998, **14**, 726-728.

58. K. R. Brown, D. G. Walter and M. J. Natan, *Chem. Mater.*, 2000, **12**, 306-313.
59. N. R. Jana, L. Gearheart and C. J. Murphy, *Langmuir*, 2001, **17**, 6782-6786.
60. S. Stoeva, K. J. Klabunde, C. M. Sorensen and I. Dragieva, *J. Am. Chem. Soc.*, 2002, **124**, 2305-2311.
61. B. L. V. Prasad, S. I. Stoeva, C. M. Sorensen and K. J. Klabunde, *Langmuir*, 2002, **18**, 7515-7520.
62. B. L. V. Prasad, S. I. Stoeva, C. M. Sorensen and K. J. Klabunde, *Chem. Mater.*, 2003, **15**, 935-942.
63. P. D. Jadzinsky, G. Calero, C. J. Ackerson, D. A. Bushnell and R. D. Kornberg, *Science*, 2007, **318**, 430-433.
64. M. W. Heaven, A. Dass, P. S. White, K. M. Holt and R. W. Murray, *J. Am. Chem. Soc.*, 2008, **130**, 3754-3755.
65. E. C. Hurst, K. Wilson, I. J. S. Fairlamb and V. Chechik, *New J. Chem.*, 2009, **33**, 1837-1840.
66. A. R. Rothrock, R. L. Donkers and M. H. Schoenfisch, *J. Am. Chem. Soc.*, 2005, **127**, 9362-9363.
67. G. A. DeVries, M. Brunnbauer, Y. Hu, A. M. Jackson, B. Long, B. T. Neltner, O. Uzun, B. H. Wunsch and F. Stellacci, *Science*, 2007, **315**, 358-361.
68. R. A. Sperling, T. Pellegrino, J. K. Li, W. H. Chang and W. J. Parak, *Adv. Funct. Mater.*, 2006, **16**, 943-948.
69. A. C. Templeton, W. P. Wuelfing and R. W. Murray, *Acc. Chem. Res.*, 2000, **33**, 27-36.
70. M. J. Hostetler, S. J. Green, J. J. Stokes and R. W. Murray, *J. Am. Chem. Soc.*, 1996, **118**, 4212-4213.
71. R. S. Ingram, M. J. Hostetler and R. W. Murray, *J. Am. Chem. Soc.*, 1997, **119**, 9175-9178.
72. M. J. Hostetler, A. C. Templeton and R. W. Murray, *Langmuir*, 1999, **15**, 3782-3789.
73. R. Guo, Y. Song, G. L. Wang and R. W. Murray, *J. Am. Chem. Soc.*, 2005, **127**, 2752-2757.
74. A. C. Templeton, M. J. Hostetler, C. T. Kraft and R. W. Murray, *J. Am. Chem. Soc.*, 1998, **120**, 1906-1911.

75. L. O. Brown and J. E. Hutchison, *J. Am. Chem. Soc.*, 1997, **119**, 12384-12385.
76. A. Ulman, *Chem. Rev.*, 1996, **96**, 1533-1554.
77. G. H. Woehrle, L. O. Brown and J. E. Hutchison, *J. Am. Chem. Soc.*, 2005, **127**, 2172-2183.
78. G. H. Woehrle and J. E. Hutchison, *Inorg. Chem.*, 2005, **44**, 6149-6158.
79. J. Noh and M. Hara, *Langmuir*, 2000, **16**, 2045-2048.
80. P. Ionita, A. Caragheorgheopol, B. C. Gilbert and V. Chechik, *J. Am. Chem. Soc.*, 2002, **124**, 9048-9049.
81. P. Ionita, A. Caragheorgheopol, B. C. Gilbert and V. Chechik, *Langmuir*, 2004, **20**, 11536-11544.
82. Y. Song, T. Huang and R. W. Murray, *J. Am. Chem. Soc.*, 2003, **125**, 11694-11701.
83. M. Zachary and V. Chechik, *Angew. Chem. Int. Ed.*, 2007, **46**, 3304-3307.
84. P. Ionita, B. C. Gilbert and V. Chechik, *Angew. Chem. Int. Ed.*, 2005, **44**, 3720-3722.
85. P. Ionita, M. Conte, B. C. Gilbert and V. Chechik, *Org. Biomol. Chem.*, 2007, **5**, 3504-3509.
86. M. Hasan, D. Bethell and M. Brust, *J. Am. Chem. Soc.*, 2002, **124**, 1132-1133.
87. P. Ionita, A. Volkov, G. Jeschke and V. Chechik, *Anal. Chem.*, 2008, **80**, 95-106.
88. V. Chechik, H. J. Wellsted, A. Korte, B. C. Gilbert, H. Caldararu, P. Ionita and A. Caragheorgheopol, *Faraday Discuss.*, 2004, **125**, 279-291.
89. V. Chechik, *J. Am. Chem. Soc.*, 2004, **126**, 7780-7781.
90. M. Montalti, L. Prodi, N. Zaccheroni, R. Baxter, G. Teobaldi and F. Zerbetto, *Langmuir*, 2003, **19**, 5172-5174.
91. A. Kassam, G. Bremner, B. Clark, G. Ulibarri and R. B. Lennox, *J. Am. Chem. Soc.*, 2006, **128**, 3476-3477.
92. K. A. Peterlinz and R. Georgiadis, *Langmuir*, 1996, **12**, 4731-4740.
93. R. Georgiadis, K. P. Peterlinz and A. W. Peterson, *J. Am. Chem. Soc.*, 2000, **122**, 3166-3173.
94. D. Yan, J. A. Saunders and G. K. Jennings, *Langmuir*, 2002, **18**, 10202-10212.
95. A. Caragheorgheopol and V. Chechik, *PCCP*, 2008, **10**, 5029-5041.

96. R. L. Donkers, Y. Song and R. W. Murray, *Langmuir*, 2004, **20**, 4703-4707.
97. A. Kumar and G. M. Whitesides, *Appl. Phys. Lett.*, 1993, **63**, 2002-2004.
98. C. S. Weisbecker, M. V. Merritt and G. M. Whitesides, *Langmuir*, 1996, **12**, 3763-3772.
99. C. B. Gorman, H. A. Biebuyck and G. M. Whitesides, *Chem. Mater.*, 1995, **7**, 252-254.